SC/67B/HIM/02

Modelling the spatial dynamics of Maui dolphins using individual based models

Monique de Jager, Geerten Hengeveld, Wolf Mooij, Elisabeth Slooten

INTERNATIONAL
WHALING COMMISSION

Modelling the spatial dynamics of Maui dolphins using individual based models

Monique de Jager[1], Geerten Hengeveld[1], Wolf Mooij[2], Elisabeth Slooten[3]

[1]Biometris, Wageningen University & Research, Droevendaalsesteeg 1,

6708PB Wageningen, Netherlands.

[2]Aquatic ecology, Netherlands Institute of Ecology (NIOO-KNAW), Droevendaalsesteeg 10,

6708 PB, Wageningen, Netherlands.

[3]Zoology Department, Otago University, 340 Great King Street, PO Box 56, Dunedin 9054,

New Zealand.

Abstract

The current anthropogenic impacts on nature necessitate more research for nature conservation and restoration purposes. To answer ecological and conservation questions concerning endangered species, individual based modelling is an obvious choice. Individual based models provide reliable results that can be used to predict the effects of different future conservation strategies, once calibrated correctly. However, proper parameterization of these models is challenging and time consuming. Here, we calibrate an individual based model of Maui dolphin movement, which generates Maui dolphin probability distribution maps. We used sighting data for validation of the chosen parameter combinations. For each simulation run, collected simulated data was compared to the empirical survey data, resulting in BoF estimates. First, each of four uncertain parameters was tested in a one-at-a-time sensitivity analysis. Three of the four parameters had a significant effect on the model's BoF. Second, different combinations of these three parameters were simulated. Using BoF on four different aspects of dolphin behaviour, we estimated the most likely parameter combinations. With optimized parameter values, Maui dolphin probability distribution maps were created, which can be used for conservation efforts. Using this approach, one is able to reliably calibrate an individual based model to fit the natural population that it should simulate.

Introduction

For the conservation of species vulnerable to extinction, it can be useful to explore the effectiveness of different restoration scenarios. Predicting the effects of different protection measures is of great importance, as policy makers can adjust their actions accordingly and adopt the management actions that will provide the best possible outcome (Cash et al. 2002). To deliver high quality predictions for possible scenarios, models are needed that represent the study system in a credible, salient, and legitimate fashion (Cash et al. 2002). Yet, many ecological questions are too complex for simple deduction or successful modelling with spatially implicit population models. Custom-made individual based models (IBMs) are often the best analysis tool for these kinds of questions.

A very urgent case in which high quality model projections are needed is that of the Maui dolphin (*Cephalorhynchus hectori maui*). The Maui dolphin is, with its current estimated population size of 63 individuals (95% CI 57-75; Baker et al. 2016), classified as critically endangered by the IUCN (Reeves et al. 2008). The declining population (Martien et al. 1999; Slooten et al. 2000; Baker et al. 2013a; Wade et al. 2014) that was once distributed along the west and south coasts of New Zealand's North Island (Du Fresne 2010; Dawson et al. 2001) is now restricted to a much smaller area of approximately 300km along the west coast, with most recent sightings within an area of about 140km length (Oremus et al. 2012). Besides their small coastal geographic range and population size, Maui dolphins have a slow reproduction rate, which makes them extremely vulnerable to extinction (Davidson et al. 2012). Although the New Zealand government has increased restrictions to fishing activities in a zone along the west coast after the death of a Maui dolphin in 2012 (Hamner,

Constantine, et al. 2014), current restrictions are not yet sufficient to result in population recovery.

Spatially implicit, population level models have successfully demonstrated the link between the Maui dolphin population decline and gillnet fishing (Martien et al. 1999; Slooten et al. 2000; Baker et al. 2013a; Wade et al. 2014), brought insight in the maximum by-catch that can be supported (Wade 1998; Wade et al. 2014), and have prompted policy measures (Slooten and Lad 1991; Martien et al. 1999; Slooten et al. 2000; Burkhart and Slooten 2003; Slooten and Dawson 2010; Slooten and Davies 2012). However, population level models do not predict where and when these policy measures should be in place. To be able to provide policy advice at high spatial resolutions, spatially explicit, individual based models are needed.

We developed a tailor-made individual based model of Maui dolphin movement, which can later be used to project the impact of fishing activities on the Maui dolphin population under alternative policy scenarios (e.g. van Beest et al. 2017; Nabe-Nielsen et al. 2018). We model hourly movement of individual dolphins at a 1 km^2 resolution for a duration of 90 days, to account for the small spatial and temporal scales at which dolphin behaviour and human impacts occur in real life. This model will be useful for (i) spatially explicit modelling of interactions between fishery activities and dolphins and (ii) informing the spatially implicit models on values for parameters with high spatial and temporal sensitivity. Dolphin behaviour in our model is based on bathymetry, social drivers, and internal drivers. Because accurate data on the distribution and dynamics of prey species is insufficient, foraging is not explicitly included in the model.

Two of the downsides of spatially explicit individual based modelling are that it is computationally and data intensive (Grimm and Railsback 2005). Each run of a well thought-out model requires at least several minutes to weeks in extreme cases, while simple population models may take seconds or less. Due to these long running times, parameter estimation and model calibration become challenging. Furthermore, the data that is required to base the model on should be highly detailed at both the spatial and temporal scale (as these would be the resolutions at which behaviour and interactions are modelled in IBMs). Models that provide a good representation of a study system generally include several parameters whose value cannot be determined directly by empirical data. To calibrate a model, results from simulation runs with different combinations of parameter estimates need to be compared to real data. Yet, the number of simulation runs required for such an analysis increases exponentially with the number of parameters. Different approaches have been used to optimize model calibration, such as manual calibration, statistical calibration techniques using maximum likelihood or Bayesian approaches, or inverse modelling (Grimm and Railsback, 2005). However, calibration remains a modelling process that is often neglected, but which should be incorporated in individual based modelling to generate more accurate predictions.

Here, we demonstrate our approach of model calibration: we first used a one-at-a-time sensitivity analysis to eliminate unnecessary dimensions and regions in the parameter space and subsequently sampled orthogonally within the parameter space that was left after the sensitivity analysis. We used data on distance moved per hour, grouping behaviour, home range sizes, and depth preferences from field observations (Dawson et al. 2004; Slooten et al. 2004, 2006; Rayment et al. 2009) to calibrate our four model parameters: the move-length

distribution's exponent, the incentive to join conspecifics, the drive to remain close to the home range centre, and the importance of local ocean depth. The calibrated model also provides more detailed insight into the locations where Maui dolphins are expected to occur. This information can be used for further collection of survey data and adjustment of the protection zones (where certain fishing methods are prohibited) by the New Zealand government.

Methods

The study system: Maui dolphins

The Maui dolphin population is distributed within a small range along the west coast of the North Island of New Zealand, ranging from Maunganui Bluff to Whanganui (Slooten et al. 2005; Slooten et al. 2006; Currey et al. 2012). The model was set up to represent the habitat of Maui dolphins (Fig. 1). In the northern part of Maui dolphin's range, protection implemented in 2008 prohibits gillnetting to 7 nautical miles (nmi) offshore and trawling to a maximum of 4 nmi offshore. Further south, between New Plymouth and Hawera, gillnets are banned to 2 rather than 7 nmi offshore and trawling is permitted regardless of distance from shore. The southernmost part of the Maui dolphin range, from Hawera to Whanganui remains unprotected. Dolphins range throughout the area, from the shoreline to the 100 m depth contour, and occasionally enter harbours (Rayment et al. 2011). Maui dolphins were observed to prefer inshore waters in population surveys with equal survey effort with respect to distance from shore (Slooten et al. 2004, 2006; Rayment and du Fresne 2007). Dolphin movement behaviours depend on local environmental factors, including water depth, distance to the coast and the presence of other dolphins and fishing vessels (Rayment and Webster 2009; Rayment et al. 2009). Maui dolphins are not attracted to gillnets, as the fish caught in

these nets are too large for them to eat (Miller et al. 2013). But they are strongly attracted to trawlers, often aggregating in large groups behind trawling vessels and diving down to the net (Rayment and Webster 2009).

The model

The objective of this paper is to accurately simulate hourly movements of Maui dolphins as a function of dolphin swimming activity, water depth, distance to their home range centres, and the distribution of nearby conspecifics. We created an individual based model to simulate the spatial distribution of dolphins over the coastal waters along the west coast of New Zealand's North Island. Figure 1 represents the area of approximately 180 by 465 km that was used for the spatial configuration of the model. Based on a detailed bathymetry map, we included average ocean depth for each 0.75 by 0.75 km grid cell.

During a simulation run, dolphins are initially placed in the landscape and iteratively move across the landscape by choosing the number of patch displacements per hour and choosing the directions of these displacements for a set number of hourly steps. First, 63 dolphins were initially placed within the simulated area. These dolphins are distributed along the coastline, with a doubled probability of initial placement in the centre area (see Fig. 1). Depth at which dolphins occur follows an exponential distribution with $\lambda = -0.05$ (based on field data). After the initial distribution of dolphins along the coastline, hourly movements were simulated at a 1km resolution. The number of moves per hour varies for each dolphin and every hour. We assumed that the distribution of the number of moves per hour can be described by a Poisson distribution, of which the scaling exponent λ is equal for all dolphins per simulation. The movement direction depends on a dolphin's preference for shallow waters, staying close to its

home range centre, and joining other dolphins. Within a 1km range, the weights of these three factors are multiplied:

$$W_{patch} = W_{depth} \cdot W_{home} \cdot W_{schooling}, \quad \text{(eq. 1)}$$

where W_{patch} is the overall weight of a patch and W_{depth}, W_{home}, and $W_{schooling}$ are the weights assigned to a patch for its depth, closeness to the focal dolphin's home range centre, and the presence of dolphins, respectively. W_{depth} follows a sigmoid function:

$$W_{depth} = (1 + 0.01^{1-d/\delta})^{-1}, \quad \text{(eq. 2)}$$

where d is the depth (in m) and δ is the depth-preference exponent, which equals the depth where $W_{depth} = 0.5$. At 0m depth, W_{depth} is kept at a constant value (0.99). W_{home} also follows a sigmoid function:

$$W_{home} = (1 + 0.01^{1-h/\eta})^{-1}, \quad \text{(eq. 3)}$$

where h is the distance to the home range centre (in km) and η is the home-range exponent, which equals the distance where $W_{home} = 0.5$. At the home range centre, W_{home} is kept at a constant value (0.99). $W_{schooling}$ is a simple step function of the number of dolphins at a patch:

$$W_{schooling} = \begin{cases} 1 & if\ n = 0, \\ 1 + \sigma & if\ n > 0 \end{cases}, \quad \text{(eq. 4)}$$

where σ is the schooling preference and n is the number of dolphins present. When running a simulation, dolphin's home range centres were set as the centre of all visited locations during a spin-up phase of 30 days, after which dolphin movements were recorded for 90 days. Afterwards, a summary including home range characteristics and distributions of hourly displacements, group sizes, and depth was created. More detailed information on the model can be found in the appended ODD (Suppl. Methods A); a summary of parameters and their descriptions is given in Table 2.

Calibration

Values of the movement exponent (λ), depth-preference exponent (δ), home-range exponent (η), and schooling preference (σ) needed to be calibrated to optimize the accuracy of the model. For this calibration process, we performed (i) a one-at-a-time sensitivity analysis (OAT) and (ii) a full assessment of simulation results from a wide range of parameter combinations. For the OAT, we simulated dolphin movement for a range of each of the four parameter values at a time, keeping the other three constant at the minimum, average and maximum values of the to-be simulated parameter space (Table 3). Using simple linear regression, we examined which of the four parameters had a significant effect on the simulation results. Those parameters that had no effect on the results would not be fully represented by a range of parameter values in the next set of simulations, thereby reducing the number of dimensions in the multidimensional parameter space. For this full assessment, we used orthogonal sampling of the different parameter values (Table 4). Simulations were replicated 50 times.

A parameter combination's accuracy for providing simulation results that closely resemble survey data was measured as a BoF (BoF) using χ^2 statistics for all recorded values that fall outside the ranges shown in table 1. Dolphin behaviour in our model is based on survey data for Maui dolphin (the North Island subspecies) and Hector's dolphin (the species as a whole). Data has been collected on i) depth preferences, ii) move length distributions, iii) grouping behaviour, and iv) home range sizes.

For depth preference BoF, the frequencies of dolphin occurrence in 0-25m, 25-50m, and 50-100m deep water observed in a model simulation was compared with those of field observations (Fig. 2a) using a χ^2-test. Depth preferences were based on population surveys with equal sampling effort with respect to distance from shore (Fig. 2a; Slooten et al. 2004, 2006; Rayment and du Fresne 2007).

For group size distribution BoF, the frequencies of groups of 1, 2, 3, 4, and > 4 observed in a simulation were compared to frequencies expected from field data (Fig. 2b). Information on Maui dolphin group size was obtained by Webster and Edwards (2008) and Oremus et al. (2012, table 1). Webster and Edwards' data was based on 13 aerial surveys conducted in 2008 alongshore the west coast of New Zealand's North Island, between Manukau Harbour and Cape Egmont. During these surveys, 23 groups of Maui dolphin were sighted. The group size distribution resulting from Webster and Edwards' study varies substantially from the distributions observed by Oremus et al. in 2010 and 2011. Their study resulted in larger group sizes than found by Webster and Edwards (2008) and was conducted by boat surveys, along the west coast of New Zealand's North Island between North Kaipara (about 100km north of Manukau Harbour) and New Plymouth (appr. 45km north of Cape Egmont). To account for all three observed group size distributions, we aim for our model's simulation results to fall within this range after calibration (table 1).

Home range BoF was calculated by comparing the minimal, mean, and maximum mean radii of the simulated dolphin home ranges to those found in literature (Stone et al. 2005; Table 1). Home range sizes have been estimated for Hector's dolphins by Stone et al. (2005) and Rayment et al. (2009). Stone et al. (2005) tagged 3 Hector's dolphins with satellite

transmitters in 2004, which provided about 3 months of GPS information. They estimated the average home range size to be between 10.35 and 13.77 km, with minimum mean home range sizes between 9.91 and 13.33 km and maximum mean home range sizes between 10.79 and 14.21 km. Rayment et al. (2009) used coastal photo-ID surveys in and around the Banks Peninsula Marine Mammal Sanctuary along the east coast of New Zealand's South Island. Locations of the 20 individuals with the largest numbers of sightings, collected between 1985 and 2006, were used to calculate the 50 (K50) and 95 (K95) percent density estimates of their home ranges. Estimates of K50 and K95 ranged between 15.2 and 19.0 km and 44.4 and 55.0 km, respectively. Because no data on home range parameters is available for Maui dolphin and the two subspecies are very similar, we used these estimates for model calibration. Estimates of the maximum distance between sightings of individual Maui dolphins in boat surveys was 80.4 km (Hamner et al. 2012) compared to 107.4 km for Hector's dolphin (Rayment et al. 2009).

Furthermore, the frequencies of hourly displacement distances, grouped in 0-0.75km, 0.75-1.5km, 1.5-2.25km, 2.25-3km, 3-5.25km, and >5.25km, observed in a simulation was compared with field observations to calculate the hourly displacement BoF. Data on distance moved per hour (move-length) was collected during Hector's dolphin surveys for behavioural and photographic identification research (Fig. 2b; e.g. Slooten et al. 1992, 1993; Slooten 1994). The primary purpose of these surveys is to estimate survival and reproductive rates, as well as behavioural and social association data. The start and end of each dolphin encounter was used for this study to provide a distribution of estimates of distance moved per hour.

To compare χ^2-values between the different BoF measures, the values were rescaled, by which a BoF of 1 indicates a deviation double the expected value. A BoF of zero would indicate an optimal fit of the model to actual observations of Maui dolphin behaviour. Assuming BoF follows a quadratic form through the 3-parameter space, we calculated the parameter combination that minimizes the total BoF (i.e. sum of the four BoFs) using an analytical approach (Suppl. Methods B).

Interpretation

Once the model parameters were calibrated, simulations with parameter values that minimized BoF were run to generate probability distribution maps of dolphin presence in the study area. To create these maps, dolphin locations were recorded during a single season (summer). To examine the robustness of our results, we repeated simulations 100 times for each likely parameter combination, as well as for parameter combinations at the edges of the simulated parameter space.

Results

Calibration

The results of the one-at-a-time sensitivity analysis indicate which parameters are most important in terms of influencing the model's performance. The movement activity exponent λ, schooling preference σ, and home-range exponent η significantly affected the BoF of the model (Fig. 3, Table 5, and Supplementary Figs. 2-5). Taking the average BoF of the four different proxies (Fig. 3), the dolphin movement activity exponent, schooling preference, and home range exponent all significantly correlate with the average BoF in a simple linear model ($R^2 = 0.811$, df = 994, $p < 0.001$). The depth preference exponent did not have any significant

effect on the average BoF of the simulation results to the survey data ($p = 0.829$). When separating the four individual BoF components, varying the home range exponent significantly affected home range BoF ($R^2 = 0.057$, df = 994, $p < 0.001$) and group size BoF ($R^2 = 0.860$, df = 994, $p < 0.001$). The movement activity exponent had a significant effect on hourly displacement BoF ($R^2 = 0.135$, df = 994, $p < 0.001$) and home range BoF ($R^2 = 0.057$, df = 994, $p < 0.001$), whereas schooling preference significantly influenced hourly displacement BoF ($R^2 = 0.135$, df = 994, $p < 0.001$), home range BoF ($R^2 = 0.057$, df = 994, $p < 0.001$), and group size BoF ($R^2 = 0.860$, df = 994, $p < 0.001$). Varying the depth preference exponent did not result in any significant trend in BoF and was therefore kept at a constant value throughout subsequent calibration runs.

Second, we ran a total of 81900 simulations (50 repetitions of different parameter combinations) in order to locate the parameter settings that will minimize the difference between modelled and observed dolphin behaviour. BoF in hourly displacement was minimized most in simulations with $\lambda = 5.1$, $\eta = 62.2$, and $\sigma = 336$ (Table 6, Fig. 4, Suppl. Fig. 6). For home range characteristics and depth preference, the BoF landscapes were less pronounced (Fig. 4; Suppl. Figs. 7-8); most parameter combinations provided a similar BoF. The analytical solutions for home range and depth BoFs resulted in the parameter combinations $\lambda = 3.8$, $\eta = 30.1$, and $\sigma = 545$, and $\lambda = 0.8$, $\eta = 20.4$, and $\sigma = 214$, respectively (Table 6). Group size distributions resembled those observed in real Maui dolphins most when $\lambda = 3.1$, $\eta = 34.4$, and $\sigma = 328$ (Table 6, Fig. 4; Suppl. Fig. 9). To locate the parameter combinations that provide the best model of Maui dolphin behaviour, we calculated the maximum BoF of the four BoF measures, for all parameter combinations (Table 6, Fig. 5). In the simulated parameter space, BoF was minimized when $\lambda = 5.1$, $\eta = 27.5$, and $\sigma = 322$.

Interpretation

Using the parameter combination that minimized the deviation between modelled and observed dolphin behaviour ($\lambda = 5.1$, $\eta = 27.5$, and $\sigma = 322$), we estimated the area used by Maui dolphins within the study site. Figure 6 illustrates the K_{50} (red), K_{95} (orange), and K_{99} (yellow) of dolphins in 100 separate runs. Our estimates of the K_{95} and K_{99} lie well beyond the boundaries of the current marine mammal sanctuary.

To check the robustness of our model, we also ran 8 x 100 simulations with parameter combinations from the edges of the parameter space ($\lambda = 1$ or 7, $\eta = 10$ or 50, and $\sigma = 10$ or 500; Fig. 7). The poorly parameterized model simulations (with $\lambda = 1$, top panels Fig. 7) result in a more spread out dolphin distribution compared to the calibrated model.

Discussion

To promote the survival of the critically endangered Maui dolphin population, conservation policies regarding restrictions on fishing and trawling activities need to be fine-tuned on the currently only coarsely known Maui dolphin distribution. We used an individual based model to estimate the occurrence of Maui dolphins along the west coast of New Zealand's North Island and thereby predict local interactions between Maui dolphins and fishing activities. To provide high quality results, four model parameters had to be calibrated. Using a one-at-a-time sensitivity analysis, we observed that one of these parameters, the depth preference exponent, did not significantly affect any of the four BoF estimates. Exclusion of this parameter resulted in a more efficient search for the optimal parameter combination in three

dimensions. By means of orthogonal sampling of different parameter combinations, we were able to find the parameter combination which minimizes BoF for all four behavioural aspects (i.e. hourly displacement, group size, depth preference, and home range characteristics).

Results from the calibrated model demonstrate that Maui dolphins stay close to the shoreline and can be found in high densities in the areas around Kapaira Harbour and Manukau Harbour. It should be noted that, in its current form, the model does not incorporate any interactions between dolphins and vessels. The dolphin distribution estimated with the calibrated model results in most of the dolphins being found inside the gillnet restricted zone; yet the dolphin distribution extends far beyond the current limits of this area (Fig. 6). This is consistent with sightings outside the protected area, at least as far as Whanganui, with occasional sightings as far as Wellington and up the east coast of the North Island of New Zealand.

More data on dolphin and fish distribution would help to further improve the model. Fish are usually clustered in patches of high nutritional value. Dolphins subsequently search for such dense aggregations, a behaviour which is currently not incorporated in our model. Information on fish distributions would much improve the current Maui dolphin movement model.

We focus on calibrating our individual based model to observed real world patterns. In such a pattern oriented approach (Grimm et al. 2005) we need to be aware of potential interactions between processes (and their associated parameter values). Even if a direct relation exists between a single process and a pattern (e.g., movement activity process and hourly displacements), other processes (e.g. attraction by dolphins) cause interactions while

generating the pattern (de Jager *et al.* 2014). Hence, parameter values which were given at first, but interact with other modelling assumptions, should be incorporated in the calibration process as parameters of unknown value.

Our model incorporates small-scale spatial detail in the estimates of the spatial distribution of Maui dolphins that can be used to estimate the effect of human (fishery) activity on population dynamics. By calibrating the model, we increased the credibility of the simulation results, as the model mimics the observed Maui dolphin behaviour best when using the calibrated parameter values. Furthermore, the high spatial resolution of the model can increase the legitimacy of applying models in policy design.

Distribution maps generated with this model will improve the current spatial distribution estimates of the Maui dolphin population and provide key input for comparison of different conservation measures. By overlaying the estimated Maui dolphin distribution map with a map indicating current fishing activities, we can pinpoint the areas where human-dolphin interactions are most likely to cause casualties. Furthermore, for different future scenarios of protection zones, we will be able to estimate the impact on the Maui dolphin population (e.g. van Beest et al. 2017; Nabe-Nielsen et al. 2018). Calculation of the overlap between Maui dolphin habitat and fishing activity as well as predictions of future scenarios will be important future directions of research.

References

Allee, W. C. 1949. Principles of animal ecology,. Saunders Co., Philadelphia.

Baker, C. S., R. M. Hamner, J. Cooke, D. Heimeier, M. Vant, D. Steel, and R. Constantine. 2013. Low abundance and probable decline of the critically endangered Maui's dolphin estimated by genotype capture–recapture. Animal Conservation 16:224–233.

Baker, C. S., Steel, D., Hamner, R. M., Hickman, G., Boren, L., Arlidge, W., Constantine, R. 2016. Estimating the abundance and effective population size of Maui dolphins using microsatellite genotypes from 2015-2016, with retrospective matching from 2001 to 2016. Report to Department of Conservation, Wellington, New Zealand www.doc.govt.nz/pagefiles/49075/maui-dolphin-abundance-2016.pdf

Burkhart, S. M., and E. Slooten. 2003. Population viability analysis for Hector's dolphin (Cephalorhynchus hectori): a stochastic population model for local populations. New Zealand Journal of Marine and Freshwater Research 37:553–566.

Cash, D., W. C. Clark, F. Alcock, N. M. Dickson, N. Eckley, and J. Jäger. 2002. *Salience, Credibility, Legitimacy and Boundaries: Linking Research, Assessment and Decision Making* (SSRN Scholarly Paper No. ID 372280). Social Science Research Network, Rochester, NY.

Courchamp, F., T. Clutton-Brock, and B. Grenfell. 1999. Inverse density dependence and the Allee effect. Trends in Ecology & Evolution 14:405–410.

Currey, R. J. C., Boren, L. J., Sharp, B. R., Peterson, D. 2012. A risk assessment of threats to Maui's dolphins. Ministry for Primary Industries and Department of Conservation, www.doc.govt.nz/getting-involved/consultations/current/threat-management-plan-review-for-mauis-dolphin/

Davidson, A. D., A. G. Boyer, H. Kim, S. Pompa-Mansilla, M. J. Hamilton, D. P. Costa, G. Ceballos, et al. 2012. Drivers and hotspots of extinction risk in marine mammals. Proceedings of the National Academy of Sciences 109:3395–3400.

Dawson, S., F. Pichler, E. Slooten, K. Russell, and C. S. Baker. 2001. The North Island Hector's dolphin is vulnerable to extinction. Marine Mammal Science 17:366–371.

Dawson, S., E. Slooten, S. DuFresne, P. Wade, and D. Clement. 2004. Small-boat surveys for coastal dolphins: line-transect surveys for Hector's dolphins (Cephalorhynchus hectori). Fishery Bulletin 102:441–451.

de Jager, M., F. Bartumeus, A. Kolzsch, F. J. Weissing, G. M. Hengeveld, B. A. Nolet, P. M. J. Herman, et al. 2014. How superdiffusion gets arrested: ecological encounters explain shift from Levy to Brownian movement. Proceedings of the Royal Society B-Biological Sciences 281:20132605.

DeAngelis, D. L., and W. M. Mooij. 2005. Individual-based modeling of ecological and evolutionary processes. Pages 147–168 *in*Annual Review of Ecology Evolution and Systematics (Vol. 36). Annual Reviews, Palo Alto.

Du Fresne, S. 2010. Distribution of Maui's dolphin (Cephalorhynchus hectori maui) 2000-2009. DOC Research & development series 322.

Grimm, V., and S. F. Railsback. 2005. Individual-based Modeling and Ecology: (STU-Student edition.). Princeton University Press.

Grimm, V., E. Revilla, U. Berger, F. Jeltsch, W. M. Mooij, et al. 2005. Pattern-oriented modeling of agent-based complex systems: lessons from ecology. Science 310:987-991.

Hamner, R. M., M. Oremus, M. Stanley, P. Brown, R. Constantine, and C. S. Baker. 2012. Estimating the abundance and effective population size of Maui dolphins using microsatellite genotypes from 2010-2011, with retrospective matching to 2001-2007. Report to Department of Conservation, Wellington, New Zealand.

Hamner, R. M., P. Wade, M. Oremus, M. Stanley, P. Brown, R. Constantine, and C. S. Baker. 2014. Critically low abundance and limits to human-related mortality for the Maui's dolphin. Endangered Species Research 26:87–92.

Martien, K. K., B. L. Taylor, E. Slooten, and S. Dawson. 1999. A sensitivity analysis to guide research and management for Hector's dolphin. Biological Conservation 90:183–191.

Miller, E., C. Lalas, S. Dawson, H. Ratz, and E. Slooten. 2013. Hector's dolphin diet: The species, sizes and relative importance of prey eaten by Cephalorhynchus hectori, investigated using stomach content analysis. Marine Mammal Science 29:606–628.

Nabe-Nielsen, J. et al. 2018. Predicting the impacts of anthropogenic disturbances on marine populations. Conservation Letters, In Press.

Oremus, M., R. M. Hamner, M. Stanley, P. Brown, C. S. Baker, and R. Constantine. 2012. Distribution, group characteristics and movements of the Critically Endangered Maui's dolphin Cephalorhynchus hectori maui. Endangered Species Research 19:1–10.

Rayment, W., S. Dawson, E. Slooten, S. Braeger, S. D. Fresne, and T. Webster. 2009. Kernel density estimates of alongshore home range of Hector's dolphins at Banks Peninsula, New Zealand. Marine Mammal Science 25:537–556.

Rayment, W., and du Fresne, S. D. 2007. Offshore aerial survey of Maui's dolphin distribution 2007. Report to Department of Conservation.

Rayment, W., and T. Webster. 2009. Observations of Hector's dolphins *(Cephalorhynchus hectori)* associating with inshore fishing trawlers at Banks Peninsula, New Zealand. New Zealand Journal of Marine and Freshwater Research 43:911–916.

Rayment W, Dawson S, Scali S, Slooten E. 2011. Listening for a needle in a haystack: passive acoustic detection of dolphins at very low densities. Endangered Species Research 14:149–156.

Reeves, R. R., Dawson, S. M., Jefferson, T. A., Karczmarski, L., *et al.* 2008. *Cephalorhynchus hectori ssp. maui.* In: IUCN 2011. IUCN Red List of Threatened Species. Version 2011.1.www.iucnredlist.org/details/39427/0

Slooten, E., Dawson, S. M. and Lad, F. 1992. Survival rates of photographically identified Hector's dolphins from 1984 to 1988. Marine Mammal Science 8(4): 327-343.

Slooten, E., Dawson, S. M. and Whitehead, H. 1993. Associations among photographically identified Hector's dolphins. Canadian Journal of Zoology 71: 2311-2318.

Slooten, E. 1994. Behavior of Hector's dolphin: Classifying behavior by sequence analysis. Journal of Mammalogy 75: 956-964.

Slooten, E., and N. Davies. 2012. Hector's dolphin risk assessments: old and new analyses show consistent results. Journal of the Royal Society of New Zealand 42:49–60.

Slooten, E., and S. M. Dawson. 2010. Assessing the effectiveness of conservation management decisions: likely effects of new protection measures for Hector's dolphin *(Cephalorhynchus hectori).* Aquatic Conservation-Marine and Freshwater Ecosystems 20:334–347.

Slooten, E., S. M. Dawson, and W. J. Rayment. 2004. Aerial surveys for coastal dolphins: Abundance of Hector's dolphins off the South Island west coast, New Zealand. Marine Mammal Science 20:477–490.

Slooten, E., Dawson, S. M., Rayment, W. J., and Childerhouse, S. J. 2005. Distribution of Maui's dolphin, *Cephalorhynchus hectori maui*. New Zealand Fisheries Assessment Report 2005/28, 21p. Published by Ministry of Fisheries, Wellington.

Slooten, E., S. Dawson, W. Rayment, and S. Childerhouse. 2006. A new abundance estimate for Maui's dolphin: What does it mean for managing this critically endangered species? Biological Conservation 128:576–581.

Slooten, E., D. Fletcher, and B. L. Taylor. 2000. Accounting for Uncertainty in Risk Assessment: Case Study of Hector's Dolphin Mortality due to Gillnet Entanglement. Conservation Biology 14:1264–1270.

Slooten, E., and F. Lad. 1991. Population Biology and Conservation of Hector Dolphin. Canadian Journal of Zoology-Revue Canadienne De Zoologie 69:1701–1707.

Stone, G., Hutt, A., Duignan, P., Teilmann, J., Cooper, R., et al. 2005. Hector's Dolphin (*Cephalorhynchus hectori hectori*) Sattelite Tagging, Health and Genetic Assessment. Department of Conservation, Auckland Conservancy Office, New Zealand.

van Beest, F. M., L. Kindt-Larsen, F. Bastardie, V. Bartolino, and J. Nabe-Nielsen. 2017. Predicting the population-level impact of mitigating harbor porpoise bycatch with pingers and time-area fishing closures. Ecosphere 8(4):e01785. 10.1002/ecs2.1785

Webster, T., and Edwards, C. 2008. Alongshore distribution surveys for Maui dolphin—March 2008. Department of Conservation, Auckland Conservancy Office, New Zealand (unpublished). 6 p.

Tables

Table 1: Target values, obtained from field observation studies, for model output. Depth distribution data was obtained from population surveys (Slooten et al. 2004, 2006; Rayment and du Fresne 2007). We collected group size distribution data from Webster and Edwards (2008) and Oresmus et al. (2012). The home range characteristics have been estimated by Stone et al. (2005) and the distribution of hourly displacements was collected from behavioural and photo-identification surveys (Slooten et al. 1992, 1993; Slooten 1994).

Data type		**Values**
Depth distribution	0-25m	59.2 %
	25-50m	34.7 %
	50-100m	6.1 %
Group size distribution	N = 1	8.3 - 25.6 %
	N = 2	4.8 - 32.6 %
	N = 3	12.5 - 19.0 %
	N = 4	16.3 - 29.4 %
	$N \geq 5$	9.3 - 37.4 %
Home range characteristics	Minimal mean radius	9.9 - 13.3 km
	Mean mean radius	10.4 – 13.8 km
	Maximum mean radius	10.8 – 14.2 km
	K_{50}	15.2 – 19 km
	K_{95}	44.4 – 55.0 km
Hourly displacement distribution	0 – 0.75 km	25.4 %
	0.75 – 1.5 km	35.9 %
	1.5 – 2.25 km	26.7 %

2.25 – 3 km	19.8 %
3 – 5.25 km	7.2 %
≥ 5.25 km	0.5 %

Table 2: Parameter names and descriptions.

Parameter name	Description
d	depth of a patch in metres
δ	depth-preference exponent
h	distance of a patch to a dolphin's home range centre in km
η	home-range exponent
n	number of dolphins present at a patch
σ	schooling preference

Table 3: Parameter combinations used in the one-at-a-time sensitivity analysis.

Varying parameter	**λ**	**δ**	**η**	**σ**
Movement exponent (λ)	0.1-5	25, 50, 100	10, 30, 50	1, 5, 50
Depth-preference exponent (δ)	1, 3, 5	2-100	10, 30, 50	1, 5, 50
Home-range exponent (η)	1, 3, 5	25, 50, 100	2-50	1, 5, 50
Schooling preference (σ)	1, 3, 5	25, 50, 100	10, 30, 50	1-50

Table 4: Parameter values used in assessment of the full parameter space.

Parameter	**Values**
Movement exponent (λ)	1, 1.5, 2, 2.5, 3, 3.5, 4, 4.5, 5, 5.5, 6, 6.5, 7
Depth-preference exponent (δ)	50
Home-range exponent (η)	10, 15, 20, 25, 30, 35, 40, 45, 50
Schooling preference (σ)	10, 20, 30, 40, 50, 60, 70, 80, 90, 100, 125, 150, 200, 500

Table 5: Results of the linear regression models, indicating the effect of the four parameters (movement, depth preference, home-range, and schooling preference) on BoF. The depth-preference exponent had no significant linear impact on the BoF.

	Hourly displacement BoF – P-value	Home range BoF – P-value	Group size BoF P-value	Depth distribution BoF – P-value	**Average BoF – P-value**
	$R^2 = 0.135$	$R^2 = 0.057$	$R^2 = 0.860$	$R^2 = 0.003$	**$R^2 = 0.811$**
Parameter	df = 994	df = 994	df = 994	df = 994	**df = 994**
Movement exponent (λ)	< 0.001	< 0.001	0.181	0.430	**< 0.001**
Depth-preference exponent (δ)	0.559	0.776	0.530	0.790	**0.829**
Home-range exponent (η)	0.141	< 0.001	< 0.001	0.033	**< 0.001**
Schooling preference (σ)	< 0.001	< 0.001	<0.001	0.165	**< 0.001**

Table 6: Parameter values that minimize BoF, estimated with a semi-analytical solution.

BoF-test	**Movement exp.**	**Home-range exp.**	**Schooling preference**
Depth	0.8	20.4	214
Group size	3.1	34.4	328
Home range	3.8	30.1	545
Hourly displacement	5.1	62.2	336
All	**5.1**	**27.5**	**322**

Figure legends

Figure 1: Map of the study area. Yellow lines indicate the central area, where approximately 50% of all dolphins have the core of their home range.

Figure 2: Depth preference distribution and hourly displacement distribution obtained from field data (e.g. Slooten 1994; Slooten et al. 1992, 1993, 2005, 2006).

Figure 3: Results of the one-at-a-time sensitivity analyses, showing BoF averaged over simulated data fit to observed hourly displacements, group sizes, depth preference, and home range characteristics. The different coloured lines indicate sets of simulations with different parameter combinations.

Figure 4: BoFs for home range characteristics, hourly displacements, depth preference, and group size distribution for all simulation runs with home range exponent = 10 (for depth preference), 30 (for home range), 35 (for group size), and 50 (for hourly displacement), averaged per parameter combination (movement exponent ranging between 1 and 7 and schooling preference ranging between 10 and 500, here shown logarithmically). Colours indicate BoF, where dark green represents those parameter combinations that provide the most accurate representation of dolphin behaviour in the model and dark red the least. A BoF of 1 indicates a deviation from the field data that is double the average field observation. Asterisks mark the parameter combinations that minimize the four BoFs, according to a semi-analytical solution (table 6).

Figure 5: Maximum BoF of the four BoF measures averaged per parameter combination. In all panels, the movement activity exponent is displayed on the x-axis (ranging between 1 and 7) and schooling preference on the y-axes (ranging between 10 and 500, shown here logarithmically). The panels differ in home range exponent, ranging from $\eta = 10$ in the bottom left panel to $\eta = 50$ in the upper right panel. The asterisk marks the parameter combination that minimizes BoF, according to a semi-analytical solution (table 6).

Figure 6: Probability distribution of the occurrence of Maui dolphins along the west coast of New Zealand's North Island, according to our calibrated model ($\lambda = 4.1$, $\delta = 50$, $\eta = 17.6$, and $\sigma = 328$; depth BoF = 0.028, home range BoF = 0.076, Hourly displacement BoF = 0.105, and group size BoF = 0.023). The map represents the total probability distribution of 100 simulations. Colours indicate estimates of K_{50} (red), K_{95} (orange), and K_{99} (yellow). The dashed and blocked areas represent the current gillnet prohibition and trawling and gillnet prohibition zones, respectively.

Figure 7: Probability distribution of the occurrence of Maui dolphins along the west coast of New Zealand's North Island, according to our model using the parameter combinations from the edges of our simulated parameter space (λ = 1 & 7, δ = 50, η = 10 & 50, and δ = 10 & 500). From top left to bottom right, depth BoF = 0.025, 0.030, 0.026, 0.026, 0.024, 0.018, 0.031, and 0.025; home range BoF = 0.267, 0.101, 0.267, 0.157, 0.260, 0.184, 0.257, and 0.272; hourly displacement BoF = 0.390, 0.387, 0.532, 0.553, 0.385, 0.424, 0.089, and 0.103; and group size BoF = 1.236, 1.354, 0.033, 0.020, 1.220, 1.361, 0.021, and 0.050, respectively. The maps represents the total probability distributions of 100 simulations. Colours indicate estimates of K_{50} (red), K_{95} (orange), and K_{99} (yellow). The dashed and blocked areas represent the current gillnet prohibition and trawling and gillnet prohibition zones, respectively.

Figures

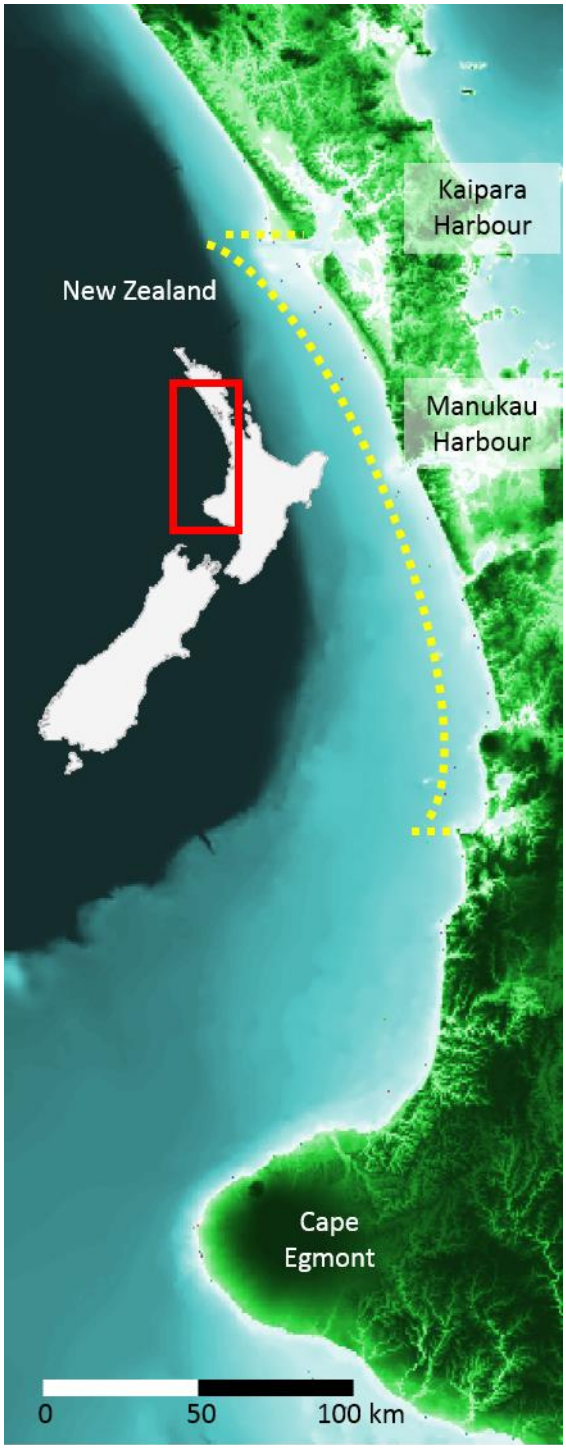

Figure 1: Map of the study area. Yellow lines indicate the central area, where approximately 50% of all dolphins have the core of their home range.

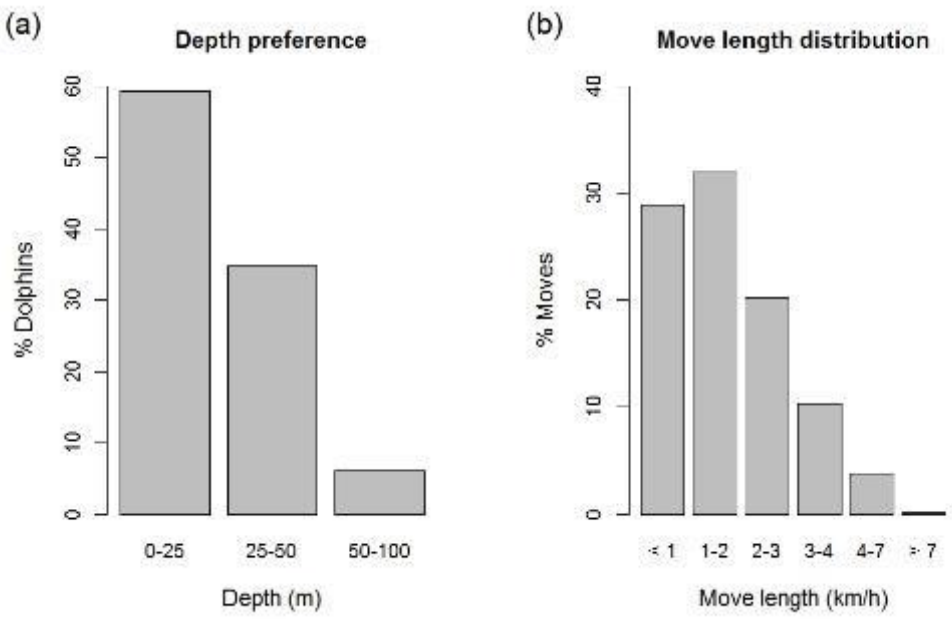

Figure 2: Depth preference distribution and hourly displacement distribution obtained from field data (e.g. Slooten 1994; Slooten et al. 1992, 1993, 2005, 2006).

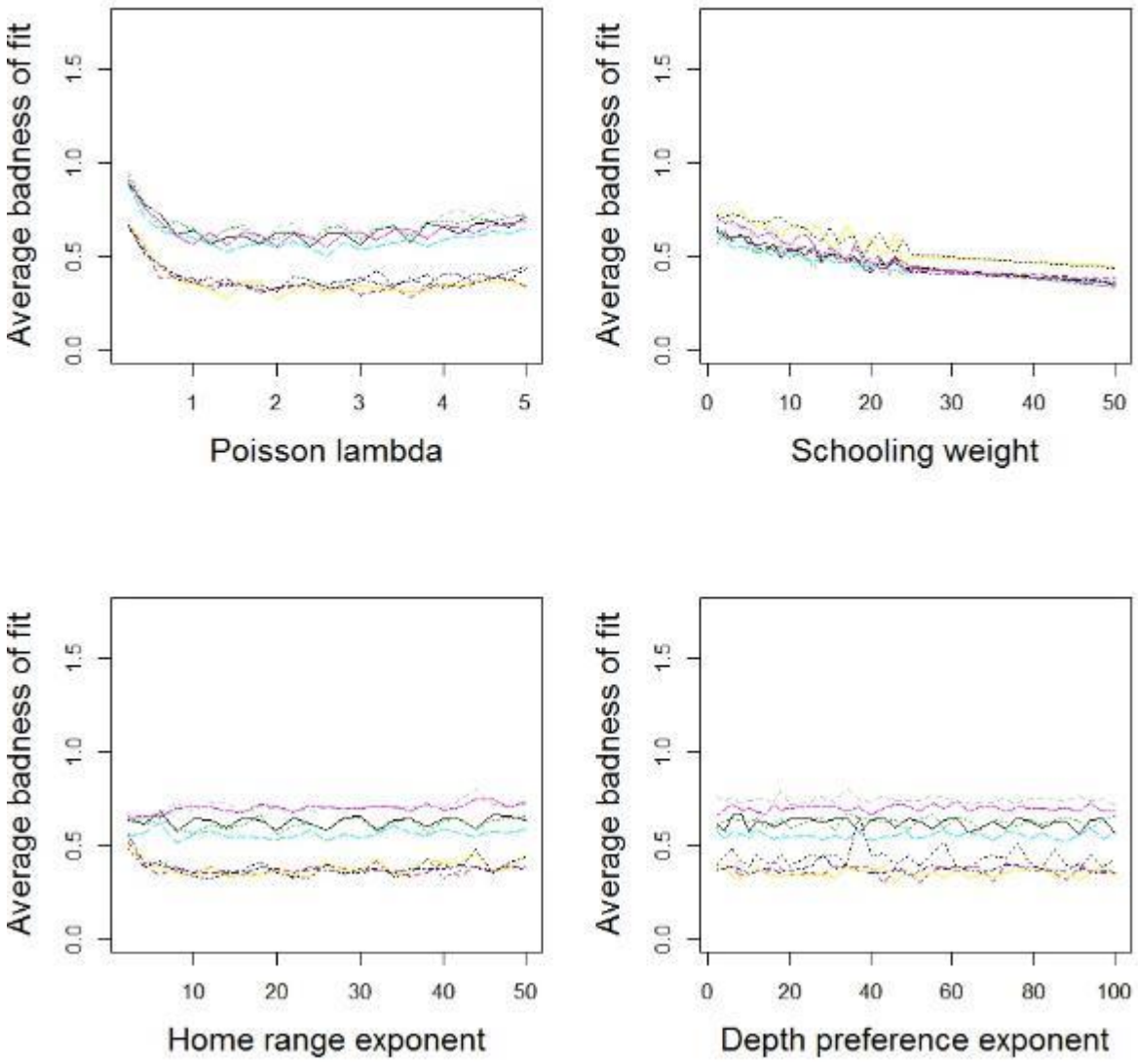

Figure 3: Results of the one-at-a-time sensitivity analyses, showing BoF averaged over simulated data fit to observed hourly displacements, group sizes, depth preference, and home range characteristics. The different coloured lines indicate sets of simulations with different parameter combinations.

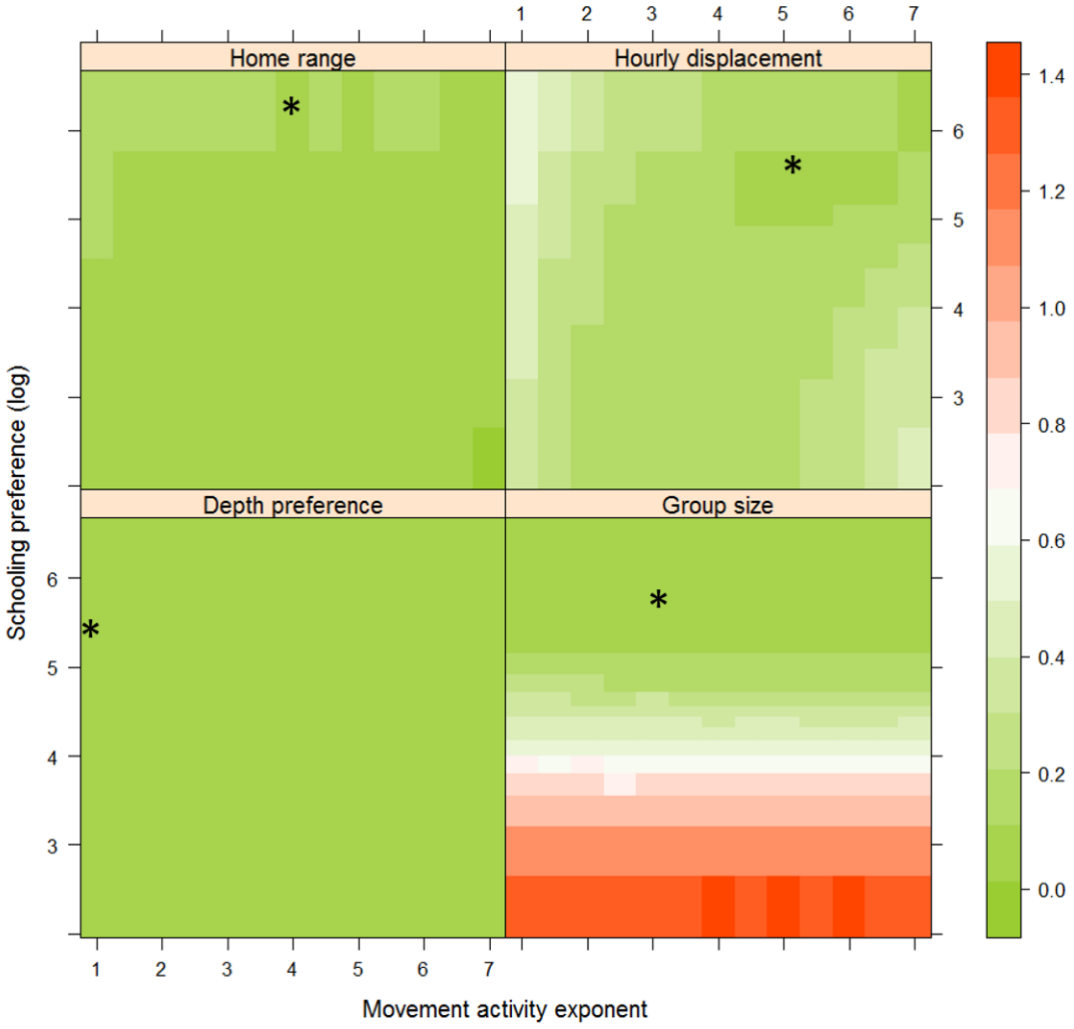

Figure 4: BoFs for home range characteristics, hourly displacements, depth preference, and group size distribution for all simulation runs with home range exponent = 10 (for depth preference), 30 (for home range), 35 (for group size), and 50 (for hourly displacement), averaged per parameter combination (movement exponent ranging between 1 and 7 and schooling preference ranging between 10 and 500, here shown logarithmically). Colours indicate BoF, where dark green represents those parameter combinations that provide the most accurate representation of dolphin behaviour in the model and dark red the least. A BoF of 1 indicates a deviation from the field data that is double the average field observation. Asterisks mark the parameter combinations that minimize the four BoFs, according to a semi-analytical solution (table 6).

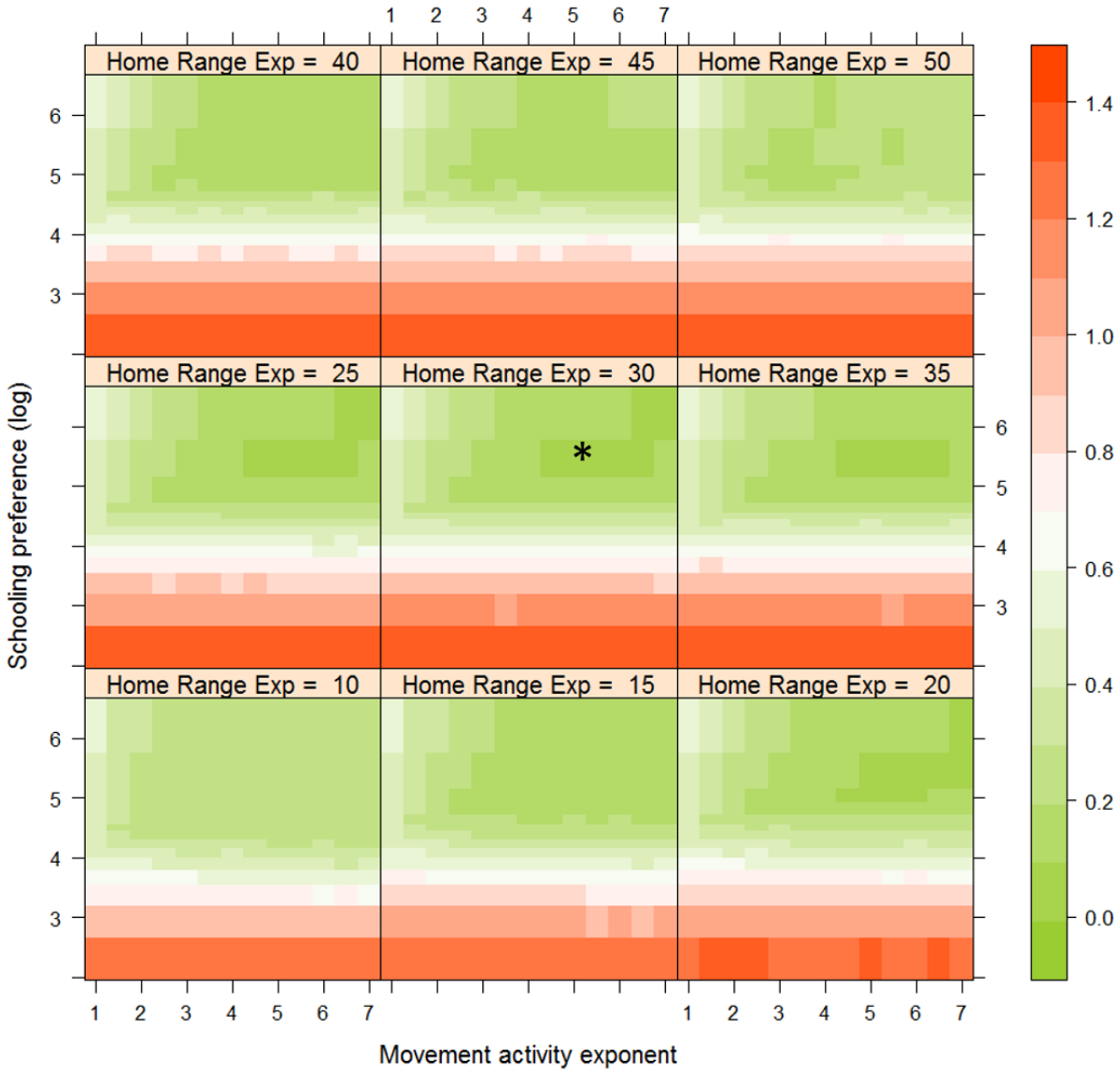

Figure 5: Maximum BoF of the four BoF measures averaged per parameter combination. In all panels, the movement activity exponent is displayed on the x-axis (ranging between 1 and 7) and schooling preference on the y-axes (ranging between 10 and 500, shown here logarithmically). The panels differ in home range exponent, ranging from $\eta = 10$ in the bottom left panel to $\eta = 50$ in the upper right panel. The asterisk marks the parameter combination that minimizes BoF, according to a semi-analytical solution (table 6).

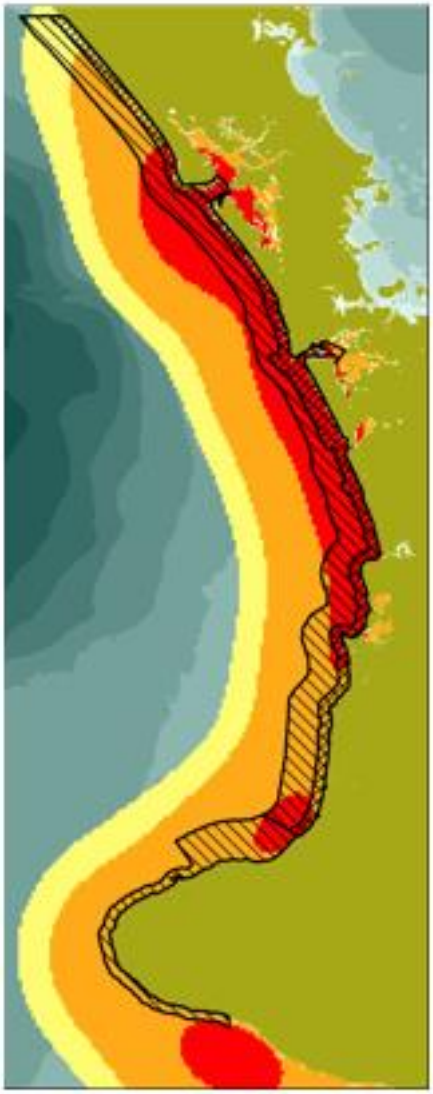

Figure 6: Probability distribution of the occurrence of Maui dolphins along the west coast of New Zealand's North Island, according to our calibrated model ($\lambda = 4.1$, $\delta = 50$, $\eta = 17.6$, and $\sigma = 328$; depth BoF = 0.028, home range BoF = 0.076, Hourly displacement BoF = 0.105, and group size BoF = 0.023). The map represents the total probability distribution of 100 simulations. Colours indicate estimates of K_{50} (red), K_{95} (orange), and K_{99} (yellow). The single-hashed and double-hashed areas represent areas where gillnets or both gillnets and trawling are prohibited, respectively.

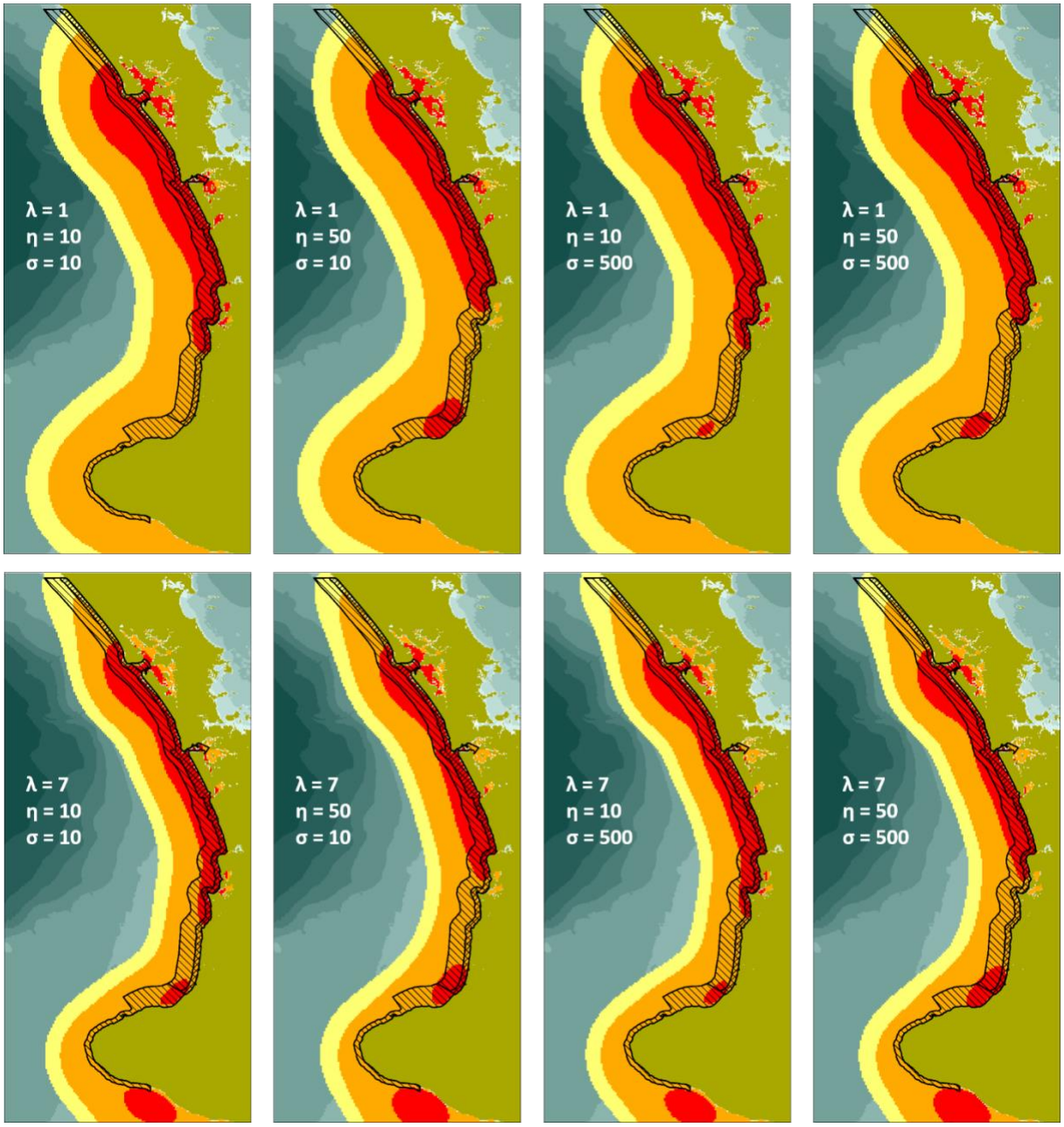

Figure 7: Probability distribution of the occurrence of Maui dolphins along the west coast of New Zealand's North Island, according to our model using the parameter combinations from the edges of our simulated parameter space (λ = 1 & 7, δ = 50, η = 10 & 50, and σ = 10 & 500). From top left to bottom right, depth BoF = 0.025, 0.030, 0.026, 0.026, 0.024, 0.018, 0.031, and 0.025; home range BoF = 0.267, 0.101, 0.267, 0.157, 0.260, 0.184, 0.257, and 0.272; hourly displacement BoF = 0.390, 0.387, 0.532, 0.553, 0.385, 0.424, 0.089, and 0.103;

and group size BoF = 1.236, 1.354, 0.033, 0.020, 1.220, 1.361, 0.021, and 0.050, respectively. The maps represents the total probability distributions of 100 simulations. Colours indicate estimates of K_{50} (red), K_{95} (orange), and K_{99} (yellow). The dashed and blocked areas represent the current gillnet prohibition and trawling and gillnet prohibition zones, respectively.

Supplementary Figures

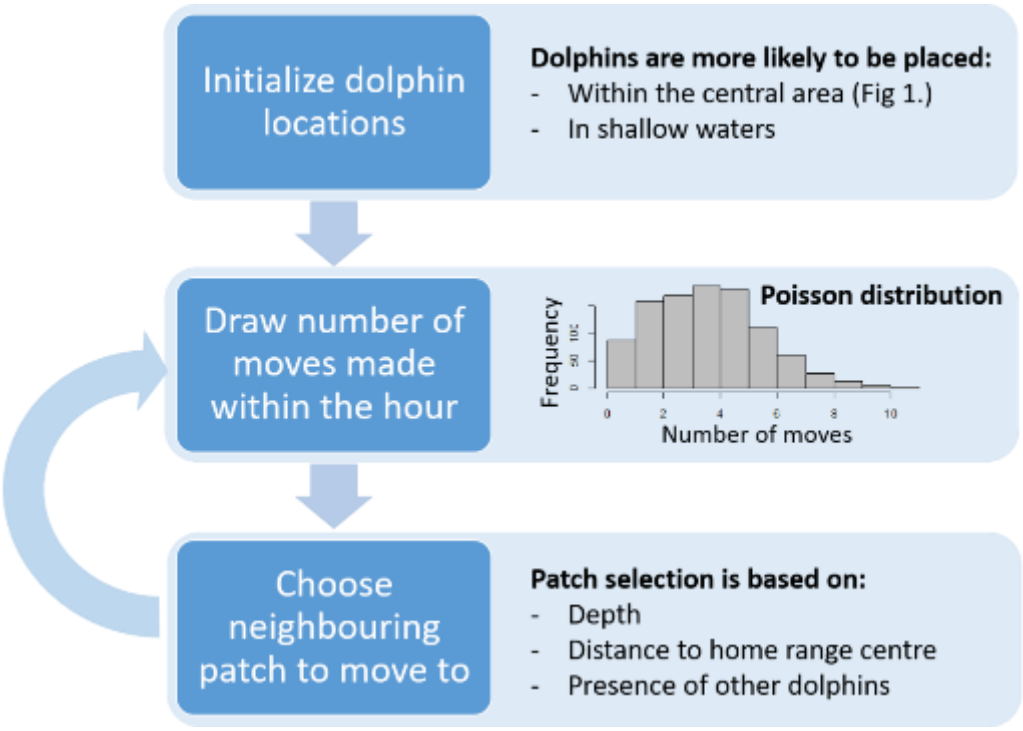

Supplementary Figure 1: Schematic illustration of the model. After initialization, dolphins iteratively move by (i) setting the number of moves that will be made to neighbouring patches within the hour-step (drawn from a Poisson distribution), and (ii) choosing a neighbouring patch to move to for the number of moves drawn in (i). Choice of destination is based on the patch depth, its distance to a dolphin's home range centre, and the presence of other dolphins.

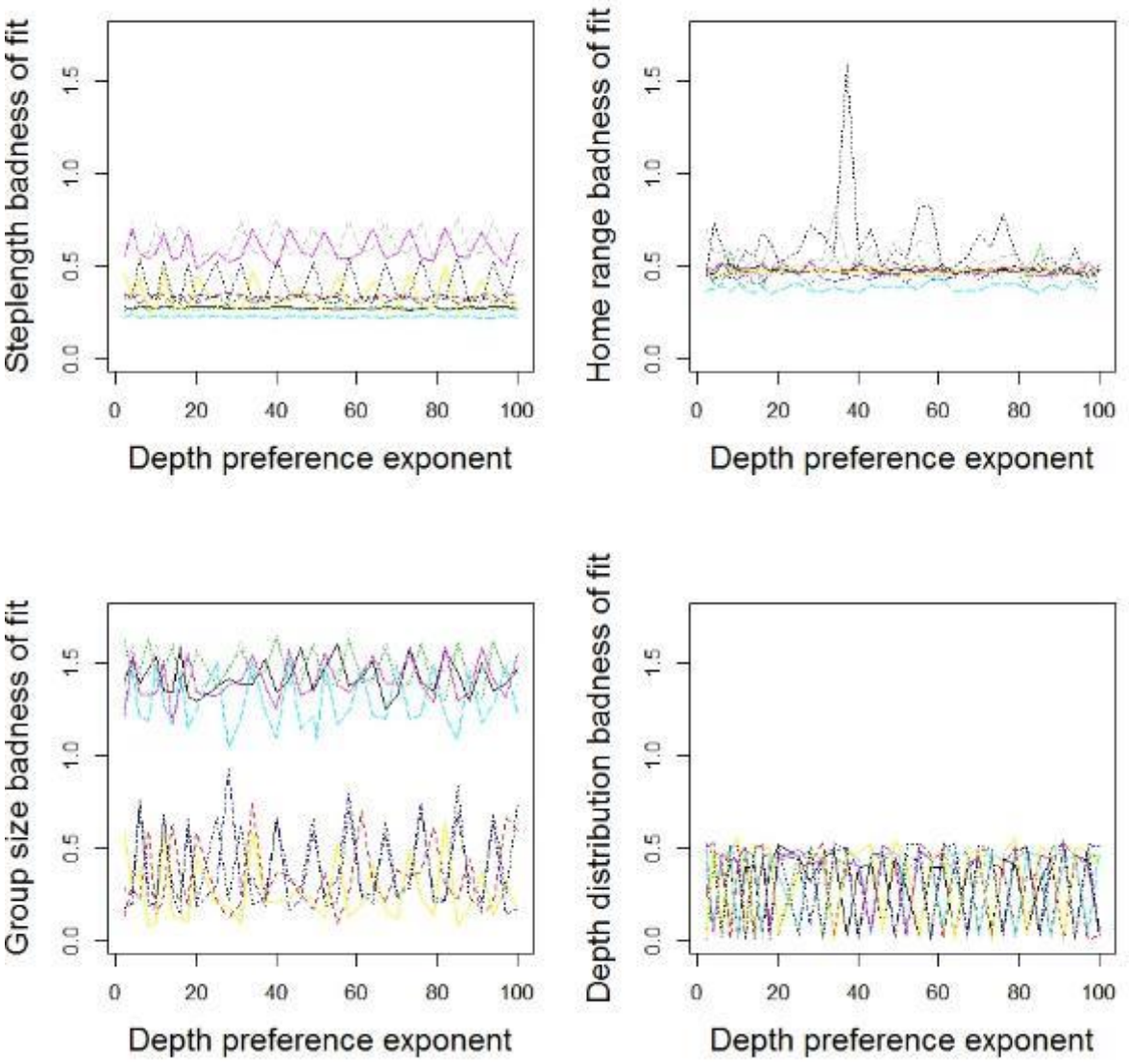

Supplementary Figure 2: BoF for step length distribution (a), home range characteristics (b), group size distribution (c), and depth distribution (d), for results of simulations varying in the depth preference exponent. No significant effects of depth preference exponent on BoF was found.

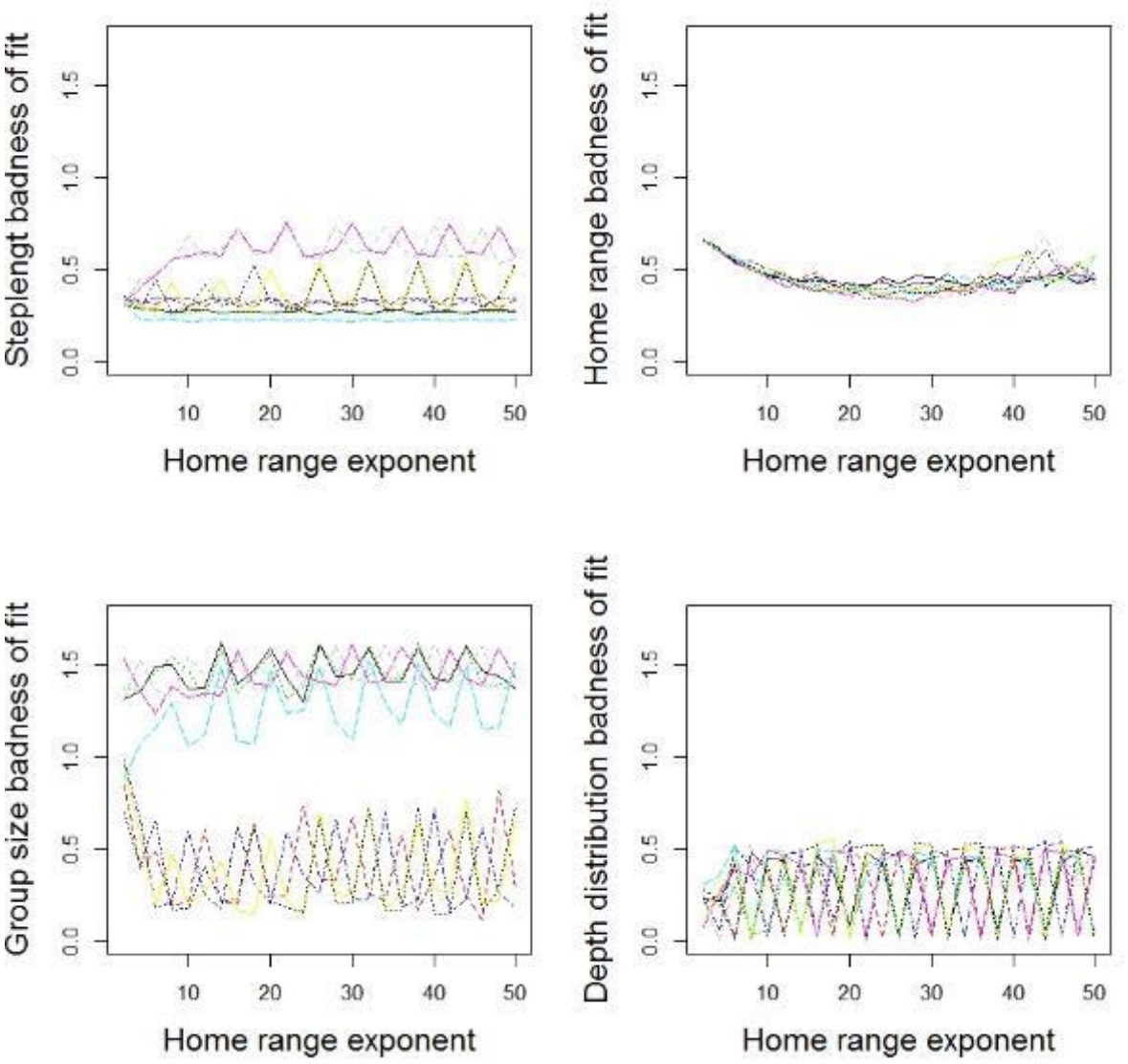

Supplementary Figure 3: BoF for step length distribution (a), home range characteristics (b), group size distribution (c), and depth distribution (d), for results of simulations varying in the home range exponent. Home range exponent has a significant effect on the home range BoF ($R^2 = 0.057$, df = 994, $p < 0.001$), the group size BoF ($R^2 = 0.860$, df = 994, $p < 0.001$), and the depth distribution BoF ($R^2 = 0.003$, df = 994, $p < 0.033$).

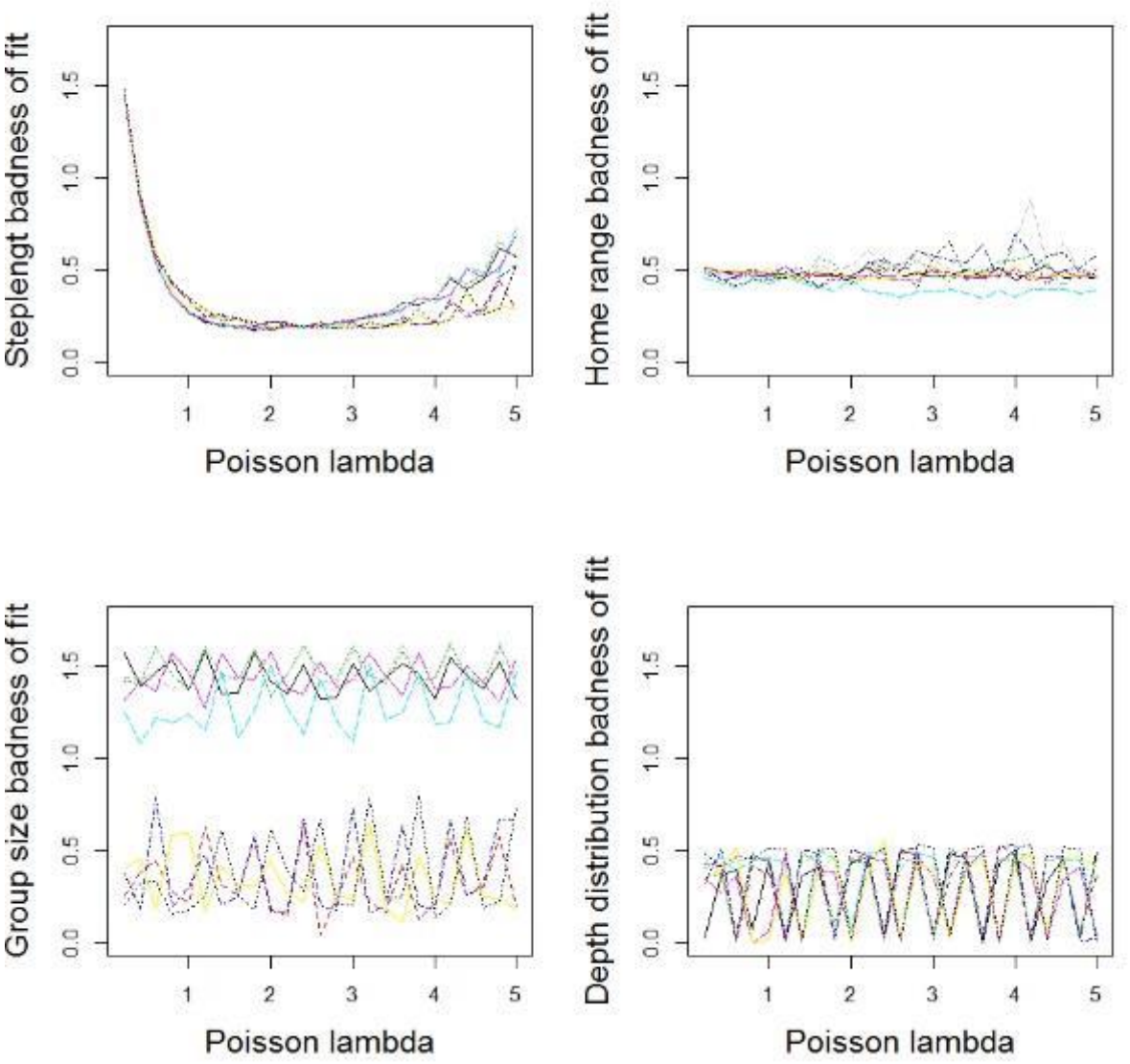

Supplementary Figure 4: BoF for step length distribution (a), home range characteristics (b), group size distribution (c), and depth distribution (d), for results of simulations varying in the movement activity exponent. The movement activity exponent has a significant effect on the step length BoF ($R^2 = 0.135$, df = 994, $p < 0.001$) and home range BoF ($R^2 = 0.057$, df = 994, $p < 0.001$).

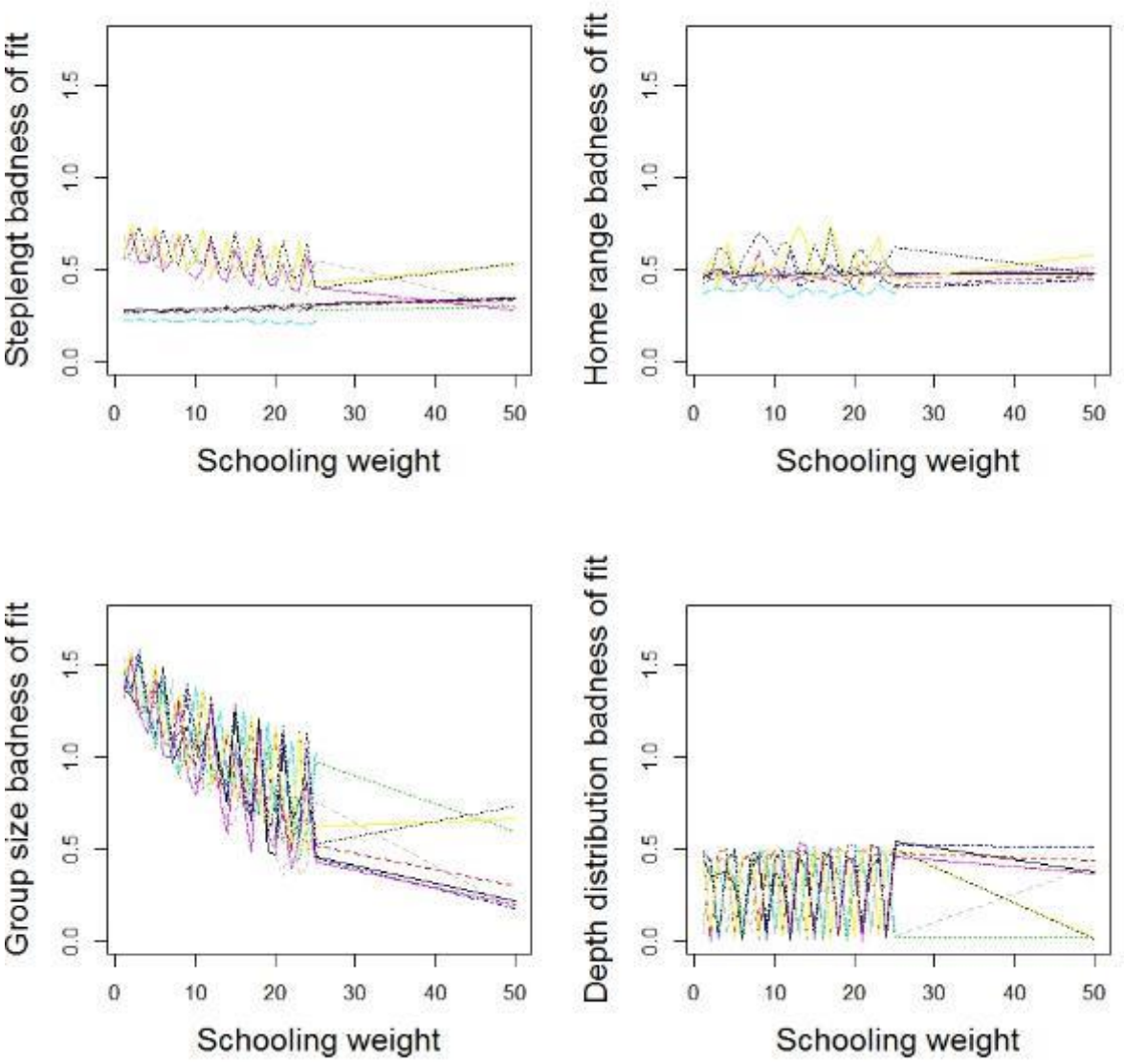

Supplementary Figure 5: BoF for step length distribution (a), home range characteristics (b), group size distribution (c), and depth distribution (d), for results of simulations varying in the schooling preference. Schooling preference has a significant effect on the step length BoF (R^2 = 0.135, df = 994, $p < 0.001$), home range BoF (R^2 = 0.057, df = 994, $p < 0.001$), and the group size BoF (R^2= 0.860, df = 994, $p < 0.001$).

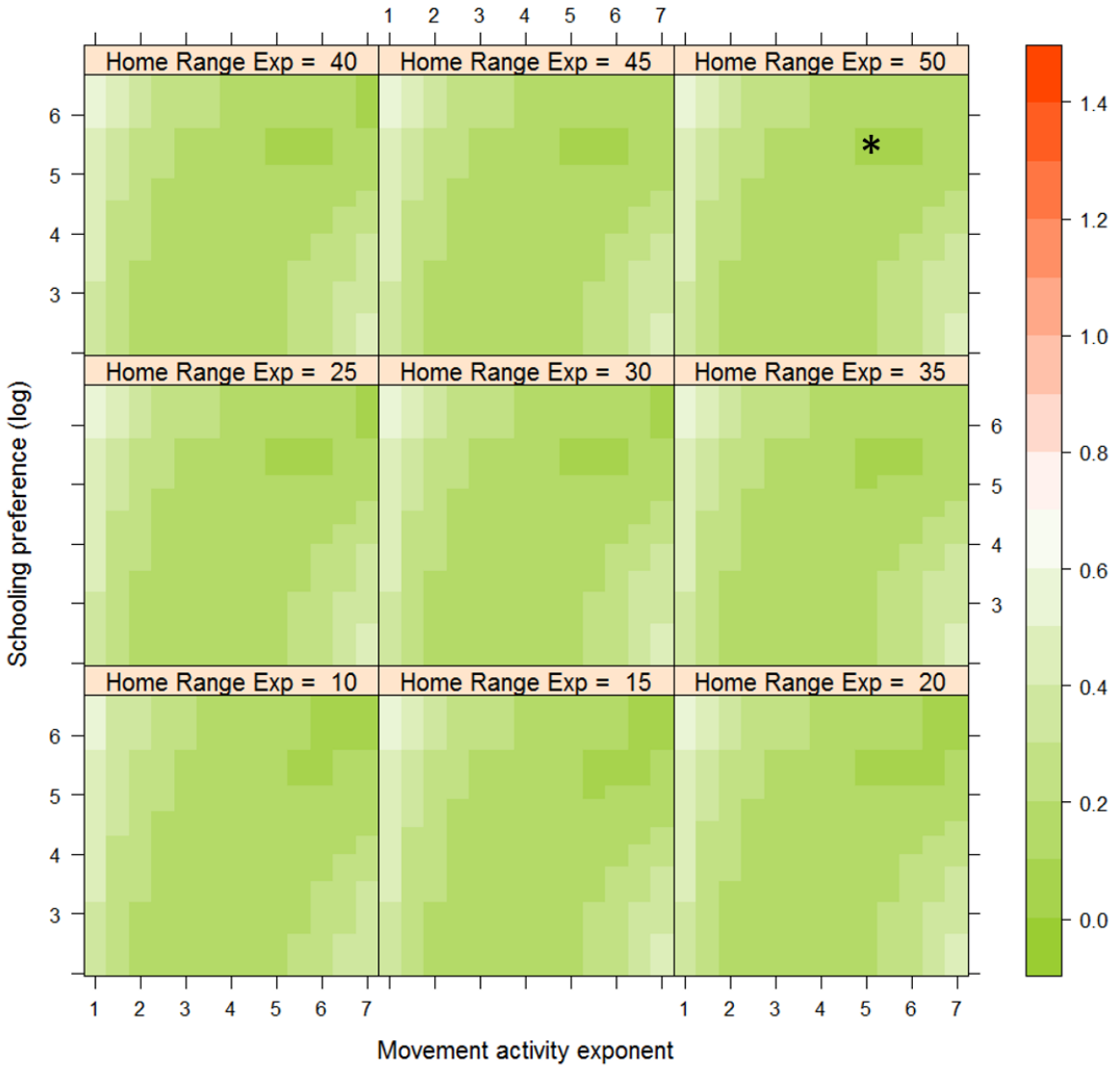

Supplementary Figure 6: BoF of hourly displacement averaged per parameter combination. In all panels, the movement activity exponent is displayed on the x-axis (ranging between 1 and 7) and schooling preference on the y-axes (ranging between 10 and 500, shown here logarithmically). The panels differ in home range exponent, ranging from $\eta = 10$ in the bottom left panel to $\eta = 50$ in the upper right panel. The asterisk marks the parameter combination that minimizes BoF, according to a semi-analytical solution (table 6).

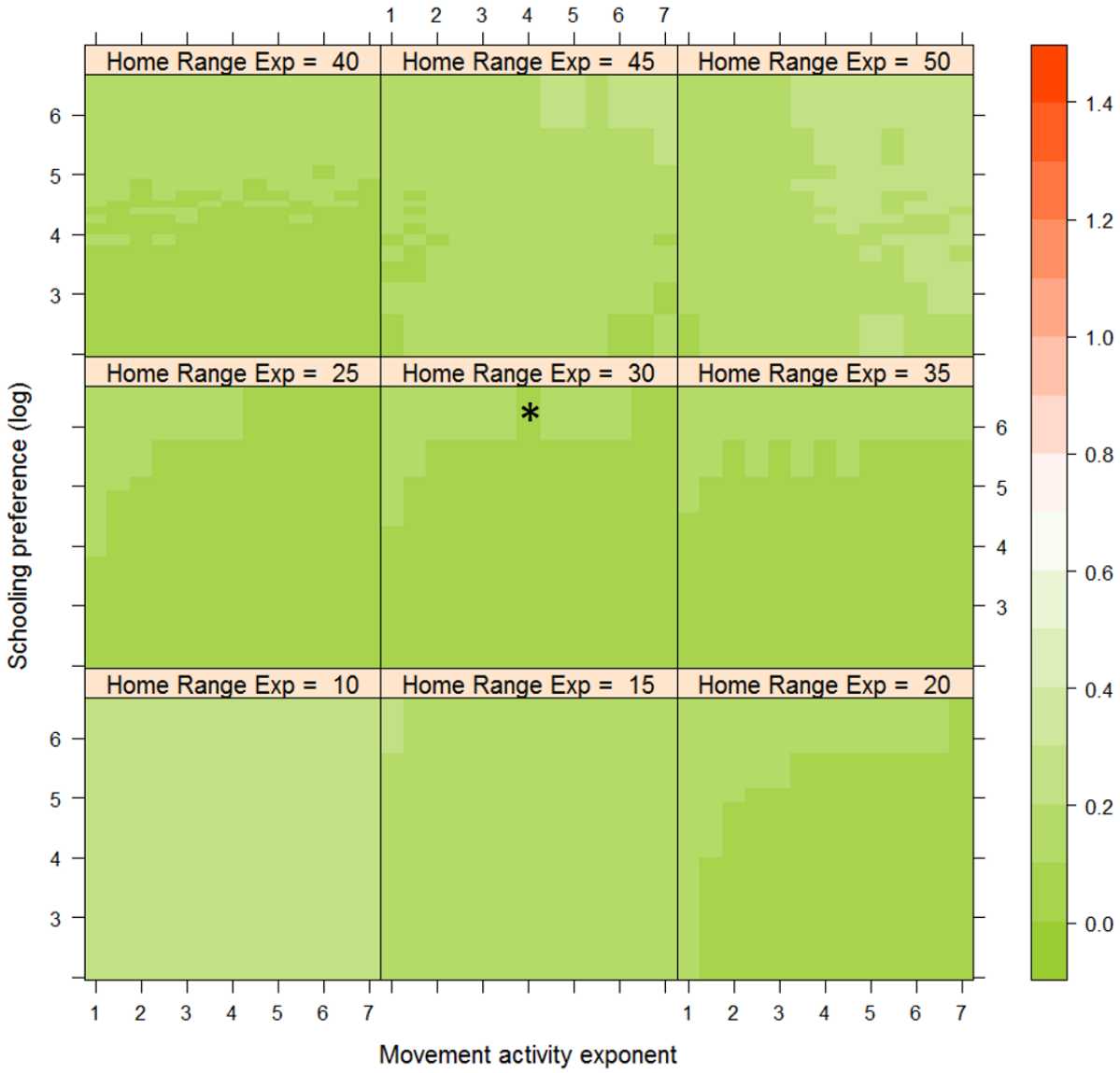

Supplementary Figure 7: BoF of home range characteristics averaged per parameter combination. In all panels, the movement activity exponent is displayed on the x-axis (ranging between 1 and 7) and schooling preference on the y-axes (ranging between 10 and 500, shown here logarithmically). The panels differ in home range exponent, ranging from η = 10 in the bottom left panel to η = 50 in the upper right panel. The asterisk marks the parameter combination that minimizes BoF, according to a semi-analytical solution (table 6).

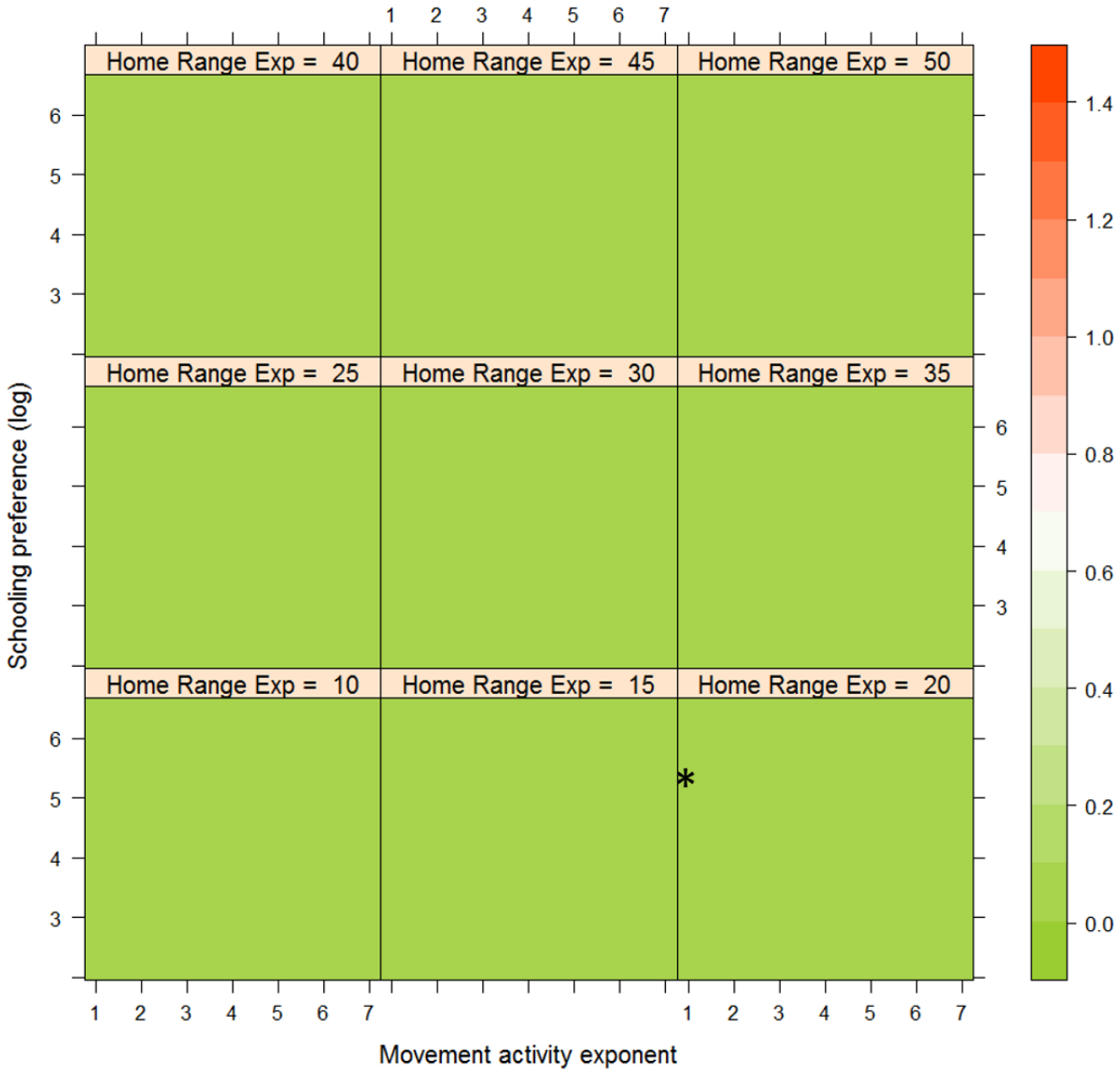

Supplementary Figure 8: BoF of depth preference averaged per parameter combination. In all panels, the movement activity exponent is displayed on the x-axis (ranging between 1 and 7) and schooling preference on the y-axes (ranging between 10 and 500, shown here logarithmically). The panels differ in home range exponent, ranging from η = 10 in the bottom left panel to η = 50 in the upper right panel. The asterisk marks the parameter combination that minimizes BoF, according to a semi-analytical solution (table 6).

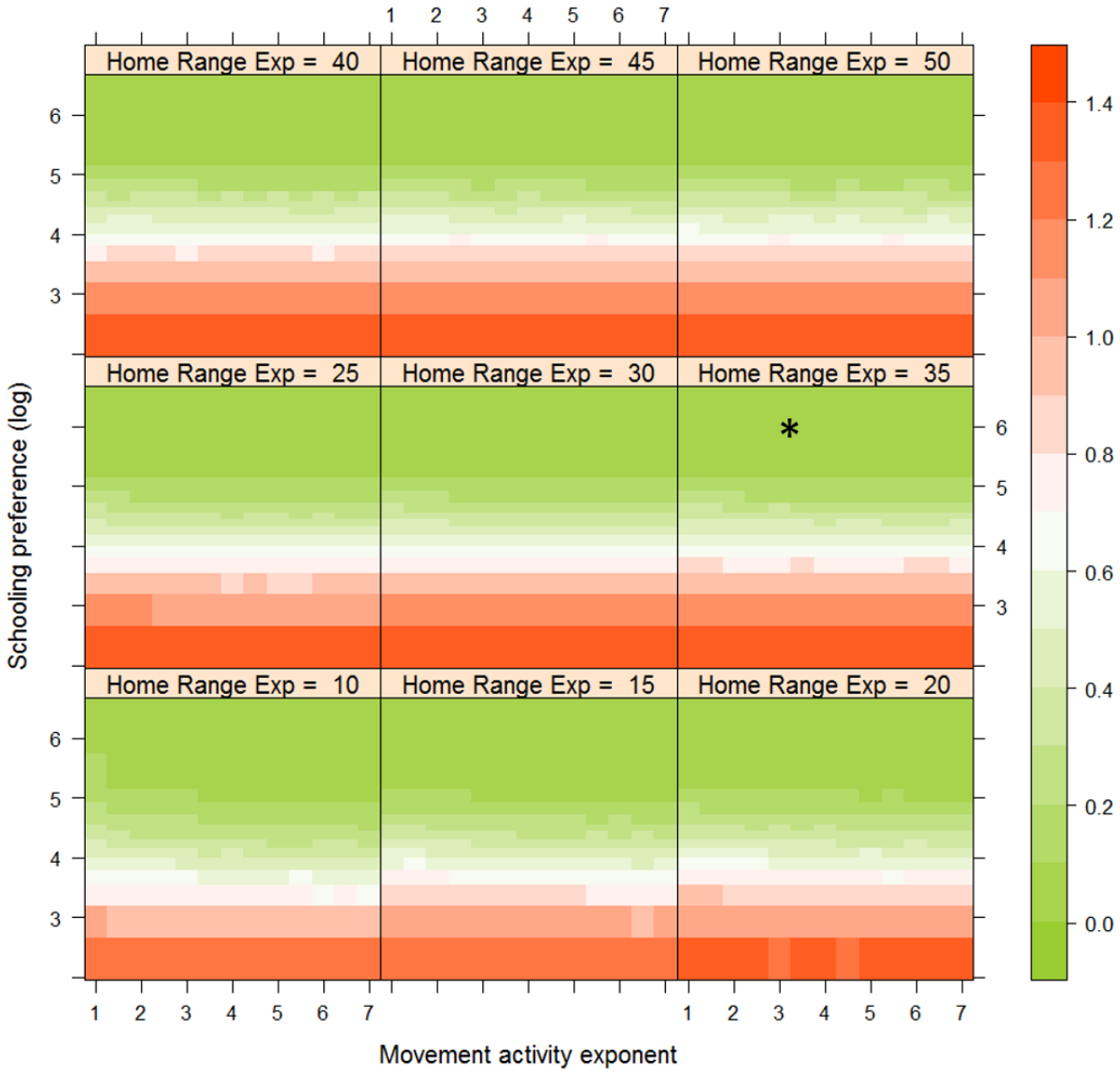

Supplementary Figure 9: BoF of group sizes averaged per parameter combination. In all panels, the movement activity exponent is displayed on the x-axis (ranging between 1 and 7) and schooling preference on the y-axes (ranging between 10 and 500, shown here logarithmically). The panels differ in home range exponent, ranging from $\eta = 10$ in the bottom left panel to $\eta = 50$ in the upper right panel. The asterisk marks the parameter combination that minimizes BoF, according to a semi-analytical solution (table 6).

Supplementary methods A: Overview, design concepts, and details (ODD) of an individual based model for Maui dolphin movement

1. Overview

Purpose

The netlogo model (Mauidolphin.nlogo) was designed to model the movements and spatial distribution of Maui dolphins over the coastal waters along the west coast of New Zealand's North Island. The model simulates hourly movements of dolphins as a function of water depth, distance from its home range centre, and the nearby presence of conspecifics.

Entities, state variables and scales

Two types of entities exist in the model: dolphins and one final collector. The dolphins are the main agents in this program, while the final collector has been created to collect, record, and write all useful data to an output file. Dolphins move around on patches, i.e. 0.75 by 0.75 km grid cells, during a set number of simulation steps.

Dolphins – Dolphins have a setup and a move procedure. During the setup procedure, the desired number of dolphins is created and distributed over the coastal waters in three steps. First, a random number is generated to indicate whether a dolphin will be positioned in the centre area, between Kaipara Harbour and Kawhia (yellow outlined area in Fig. 1), with a 50% probability, or north or south of this area (both $p = 0.25$). Second, the depth (d) of the cell at which a dolphin is randomly placed is drawn from an exponential distribution: $d = -\ln(x)/ 0.05$, where x is a random number ($0 \leq x \leq 1$) and the value 0.05 is based on an exponential fit to depth distribution data obtained from surveys with equal survey effort with respect to distance from shore (Slooten et al. 2004, 2006; Rayment and du Fresne 2007). Third, a starting location is then drawn from all cells that meet these two requirements. In the move procedure, dolphin movement is simulated at a 1km resolution. Dolphins move towards

one of their neighbouring cells based on the cells' depth, distance to the dolphins' home range centre, and the presence of conspecifics. For each cell, a weight is calculated from these three components:

$$W_{patch} = W_{depth} \cdot W_{home} \cdot W_{schooling},$$

where W_{patch} is the overall weight of a patch and W_{depth}, W_{home}, and $W_{schooling}$ are the weights assigned to a patch for its depth, closeness to the focal dolphin's home range centre, and the presence of dolphins, respectively. W_{depth} follows a sigmoid function:

$$W_{depth} = (1 + 0.01^{1-d/\delta})^{-1},$$

where d is the depth (in m) and δ is the depth-preference exponent, which equals the depth where $W_{depth} = 0.5$. W_{home} follows a sigmoid function:

$$W_{home} = (1 + 0.01^{1-h/\eta})^{-1},$$

where h is the distance to the home range centre (in km) and η is the home-range exponent, which equals the distance where $W_{home} = 0.5$. $W_{schooling}$ is a simple step function of the number of dolphins at a patch:

$$W_{schooling} = \begin{cases} 1 & if\ n = 0, \\ 1 + \sigma & if\ n > 0 \end{cases},$$

where σ is the schooling preference and n is the number of dolphins present. The total weight of a cell is used in a random biased selection of neighbouring cells to move to. The number of moves per hour is randomly drawn from a Poisson distribution, whose scaling exponent is the variable pmove. Each dolphin has a location (x-y coordinates) recorded at every time step (1 hour).

Final collector – A final collector is created to keep record of group size distributions, analyse home range characteristics, and summarize the recorded measurements on hourly

displacement distributions, depth distributions, group size distributions, and home range characteristics. Final collector writes the summarized output to a file.

Patches – The spatial units in Netlogo are the patches, which represent land or ocean surface in a 0.75 x 0.75 km resolution. The patches have the properties p_depth (the average water depth of the patch) and p_visits (an indicator of the number of hourly steps at which dolphins were present at the focal patch). There are no patch-specific actions; patches do however report their weights to dolphins in the dolphin move procedure.

Global parameters – Dolphin-specific global parameters, defined on the GUI as sliders or input fields, are: pmove (the movement activity exponent λ which determines the number of moves a dolphin makes per hour, by random selection of a number from a Poisson distribution with exponent λ), home-range-exponent (η, the parameter that is used to describe the patch home range weight), depth-preference-exponent (δ, the parameter that is used to describe patch depth weight), and pjoin (σ, the parameter that is used to describe patch dolphin weight). These parameters influence dolphin movement activity (λ) and direction (η, δ, and σ; see section 'Dolphins' above).

Scales – The spatial configuration of the patches in the netlogo model is set to a 286 km by 600 km GIS map of the west coast of the North Island of New Zealand. The spatial units are proportioned to 0.75 by 0.75 km and the temporal grain is 1 hour. This means that the standard move procedure takes time steps of an hour. Although no hard run limit is set, the model is designed to cover the movements of dolphins over a single season. No difference is made in the model between day and night as dolphins are active both day and night.

Process overview and scheduling

The model is run through the move procedure each hour, in which dolphins are displaced. For each dolphin, the following procedure is used:

- A random number of steps to be taken to neighbouring patches within an hour is drawn from a Poisson distribution with movement activity exponent λ.
- For each step, a neighbouring patch to move towards is selected using a biased random selection procedure, based on the patch weight of the neighbouring patches (see Table 2).
- Land patches (p_depth < 0) are excluded from the list of neighbouring patches to potentially move to.

The go-season procedure consists of three phases:

- First, dolphins move around during the spin-up phase, in which the home range centre is determined as the centre location of a dolphin's movements. The length of the spin-up phase can be set using the slider in the interface.
- Second, movements are simulated for 90 days (one "season"). Simulation length in days can also be adjusted with a slider in the interface.
- Third, data (i.e. group size distribution, hourly displacement length distribution, home range characteristics, and depth distribution) is collected for all movements during the simulation by the FinalCollector.

The go-season-dolphin-distribution procedure consists of the following phases:

- For a number of iterations given by the number-of-seasons slider on the GUI, (i) an initial setup of dolphin locations is made, (ii) a spin-up phase is run (in which dolphins' home range centres are set), and (iii) movements are simulated for a number of iterations given by the season-length slider in the GUI.
- After the simulation, the number of times hourly displacements ended up on a certain patch (i.e. p_visits) is written to a file for all patches with p_visits > 0, by the FinalCollector. This file can be used to make estimates of K99, K95, and K50

distribution maps in R ('ProbabilityDistributionMaker2.1.R' in 'Output/Probability distribution').

2. Design concepts

Here, we highlight the design concepts of the model:

- Dolphins are aware of conspecifics, ocean depth, and distance from the home range centre within a detection radius of approximately < 1 km, thereby spanning the 8 neighbouring patches.
- Dolphins are attracted to other dolphins, shallow waters, and prefer to stay close to their home range centres.
- The starting position and displacements of dolphins are stochastic procedures.
- Dolphins are attracted to each other, however no additional active collective behaviour is modelled. Dolphins moving to the same location are drawn in by the same attractor.
- Dolphins keep track of their own path. At the end of the simulation, the FinalCollector uses these dolphin-specific paths to calculate home range characteristics.

3. Details

Initialization

Water depth initialization –The GIS map is based on a GIS layer showing the northwest of the North Island of New Zealand with the outline of the North Island and information on water depth. The GIS data are stored in txt files in the subfolder Rasters. These are asci grids with a custom read-function.

Dolphin location initialization – There are 63 dolphins present in the modelled area; the number of simulated dolphins can be set using a slider in the interface. During the setup procedure, the desired number of dolphins is created and distributed over the coastal waters in three steps. First, a random number is generated to indicate whether a dolphin will be positioned in the centre area, between Kaipara Harbour and Kawhia (yellow outlined area in Fig. 1), with a 50% probability, or north or south of this area (both $p = 0.25$). Second, the depth (d) of the cell at which a dolphin is randomly placed is drawn from an exponential distribution: $d = - \ln(x)/ 0.05$, where x is a random number ($0 \leq x \leq 1$) and the value 0.05 is based on an exponential fit to depth distribution data obtained from surveys with equal survey effort with respect to distance from shore (Slooten et al. 2004, 2006; Rayment and du Fresne 2007). Third, a starting location is then drawn from all cells that meet these two requirements.

Dolphin movement – For dolphin movement, the parameters are set in sliders and input boxes in the interface and are thereby user defined.

Input

GIS data for bathymetry was used as input for the model (see initialization).

Supplementary Methods B

Assuming BoF follows a quadratic form through the 3-parameter space, we calculated the parameter combination that minimizes the total BoF (i.e. sum of the four BoFs) using an analytical approach.

Our quadratic form lies in a three dimensional space, based on the home-range exponent, movement activity exponent, and schooling preference. Here we refer to these parameters as x_1, x_2, and x_3 for simplicity. Let the parameter values that minimize BoF be α_1, α_2, and α_3. These are the deviations from the centre point (0,0,0), at which the quadratic form should have its minimum. The quadratic form in three dimensions with an offset of the centre point can be written as:

$$y = [(x_1 - \alpha_1)\,(x_2 - \alpha_2)\,(x_3 - \alpha_3)] \begin{bmatrix} a & b & c \\ b & d & e \\ c & e & f \end{bmatrix} \begin{bmatrix} (x_1 - \alpha_1) \\ (x_2 - \alpha_2) \\ (x_3 - \alpha_3) \end{bmatrix}, \qquad \text{(eq. 1)}$$

which can be rephrased as:

$$y = \underbrace{a\alpha_1 + d\alpha_2 + f\alpha_3 + 2b\alpha_1\alpha_2 + 2c\alpha_1\alpha_3 + 2e\alpha_2\alpha_3}_{\beta_0} + \underbrace{-2(a\alpha_1 + b\alpha_2 + c\alpha_3)}_{\beta_1} \cdot$$

$$x_1 + \underbrace{a}_{\beta_2} \cdot x_1^2 + \underbrace{-2(b\alpha_1 + d\alpha_2 + e\alpha_3)}_{\beta_3} \cdot x_2 + \underbrace{d}_{\beta_4} \cdot x_2^2 + \underbrace{-2(c\alpha_1 + e\alpha_2 + f\alpha_3)}_{\beta_5} \cdot x_3 +$$

$$\underbrace{f}_{\beta_6} \cdot x_3^2 + \underbrace{2b}_{\beta_7} \cdot x_1x_2 + \underbrace{2c}_{\beta_8} \cdot x_1x_3 + \underbrace{2e}_{\beta_9} \cdot x_2x_3. \qquad \text{(eq. 2)}$$

We use a linear regression model in R to estimate β_0, β_1, ... , β_9. These estimates are used to calculate α_1, α_2, and α_3 with the following approach:

$\beta_1 = -2\beta_2\alpha_1 - \beta_7\alpha_2 - \beta_8\alpha_3$, hence,

$$\alpha_1 = \frac{\beta_1 + \beta_7\alpha_2 + \beta_8\alpha_3}{-2\beta_2}. \qquad \text{(eq. 3)}$$

$\beta_3 = -\beta_7\alpha_1 - 2\beta_4\alpha_2 - \beta_9\alpha_3$, hence,

$$\alpha_1 = \frac{\beta_3 + 2\beta_4\alpha_2 + \beta_9\alpha_3}{-\beta_7}. \quad \text{(eq. 4)}$$

Combining eq. 3 and 4 gives:

$$\alpha_2 = k_1(2\beta_2\beta_3 - \beta_1\beta_7) + \alpha_3 k_1 \cdot (2\beta_2\beta_9 - \beta_7\beta_8), \quad \text{(eq. 5)}$$

where $k_1 = \frac{1}{\beta_7^2 - 4\beta_2\beta_4}$.

$\beta_5 = -\beta_8\alpha_1 - \beta_9\alpha_2 - 2\beta_6\alpha_3$, hence,

$$\alpha_1 = \frac{\beta_5 + \beta_9\alpha_2 + 2\beta_6\alpha_3}{-\beta_8}. \quad \text{(eq. 6)}$$

Combining eq. 4 and 6 gives:

$$\alpha_2 = k_2(\beta_5\beta_7 - \beta_3\beta_8) + \alpha_3 k_2 \cdot (2\beta_6\beta_7 - \beta_8\beta_9), \quad \text{(eq. 5)}$$

where $k_2 = \frac{1}{2\beta_4\beta_8 - \beta_7\beta_9}$.

We now calculate the last minimizing parameter value, α_3, from eq. 3 and 5:

$$\alpha_3 = k_3(k_2(\beta_5\beta_7 - \beta_3\beta_8) - k_1 \cdot (2\beta_2\beta_3 - \beta_1\beta_7)), \quad \text{(eq. 6)}$$

where $k_3 = \frac{1}{k_1(2\beta_2\beta_9 - \beta_7\beta_8) - k_2(2\beta_6\beta_7 - \beta_8\beta_9}$.